

Review

Open Access



Understanding the role of interfaces in solid-state lithium-sulfur batteries

Tao Tao^{1,*}, Zhijia Zheng¹, Yuxuan Gao¹, Baozhi Yu², Ye Fan², Ying Chen², Shaoming Huang¹, Shengguo Lu¹

¹School of Materials and Energy, Guangdong University of Technology, Guangzhou 510006, Guangdong, China.

²Institute for Frontier Materials, Deakin University, Waurn Ponds 3216, Australia.

*Correspondence to: Dr. Tao Tao, School of Materials and Energy, Guangdong University of Technology, Guangzhou 510006, Guangdong, China. E-mail: taotao@gdut.edu.cn

How to cite this article: Tao T, Zheng Z, Gao Y, Yu B, Fan Y, Chen Y, Huang S, Lu S. Understanding the role of interfaces in solid-state lithium-sulfur batteries. *Energy Mater* 2022;2:200036. <https://dx.doi.org/10.20517/energymater.2022.46>

Received: 16 Aug 2022 **First Decision:** 6 Sep 2022 **Revised:** 23 Sep 2022 **Accepted:** 8 Oct 2022 **Published:** 21 Oct 2022

Academic Editors: Yuping Wu, Jiazhao Wang **Copy Editor:** Fangling Lan **Production Editor:** Fangling Lan

Abstract

All-solid-state lithium-sulfur batteries (ASSLSBs) exhibit huge potential applications in electrical energy storage systems due to their unique advantages, such as low costs, safety and high energy density. However, the issues facing solid-state electrolyte (SSE)/electrode interfaces, including lithium dendrite growth, poor interfacial capability and large interfacial resistance, seriously hinder their commercial development. Furthermore, an insufficient fundamental understanding of the interfacial roles during cycling is also a significant challenge for designing and constructing high-performance ASSLSBs. This article provides an in-depth analysis of the origin and issues of SSE/electrode interfaces, summarizes various strategies for resolving these interfacial issues and highlights advanced analytical characterization techniques to effectively investigate the interfacial properties of these systems. Future possible research directions for developing high-performance ASSLSBs are also suggested. Overall, advanced *in-situ* characterization techniques, intelligent interfacial engineering and a deeper understanding of the interfacial properties will aid the realization of high-performance ASSLSBs.

Keywords: All-solid-state lithium-sulfur batteries, interfacial issues, advanced strategies, solid-state electrolytes, sulfur-based cathodes

INTRODUCTION

The development of portable electronic equipment and electric vehicle technology has created a substantial



© The Author(s) 2022. **Open Access** This article is licensed under a Creative Commons Attribution 4.0 International License (<https://creativecommons.org/licenses/by/4.0/>), which permits unrestricted use, sharing, adaptation, distribution and reproduction in any medium or format, for any purpose, even commercially, as long as you give appropriate credit to the original author(s) and the source, provide a link to the Creative Commons license, and indicate if changes were made.



market demand for lithium-ion batteries, which have high energy density and good long-term cycle performance. A lithium-ion battery is mainly composed of a cathode, such as lithium cobalt oxide, lithium manganese oxide, lithium nickel manganese cobalt oxide or lithium iron phosphate, an electrolyte, a separator and an anode, such as graphite. At present, traditional Li-ion batteries cannot meet the desired storage requirements due to their limited theoretical specific capacity and safety issues^[1]. Thus, the development of novel energy storage energy systems has become a significant challenge. Lithium-sulfur batteries (LSBs) have received substantial attention due to their high energy density, environmental friendliness and low cost. However, liquid electrolyte LSBs are limited by low Coulombic efficiency and fast capacity degradation because of the polysulfide dissolution and shuttling. The toxicity and flammability of liquid electrolytes also cause safety concerns. All-solid-state lithium-sulfur batteries (ASSLSBs) are regarded as potential substitutes. ASSLSBs contain a metallic lithium-based anode, solid-state electrolyte (SSE) and sulfur-based cathode. The use of a nonflammable SSE can suppress the polysulfide dissolution, eliminate the shuttle effect and restrain the formation of lithium dendrites^[2,3]. Furthermore, ASSLSBs show additional advantages, including reduced wasted volume and net weight, low self-discharge, high operating voltages and excellent thermal stability^[4-6]. A comparison between liquid electrolyte-based LSBs and ASSLSBs is shown in [Table 1](#).

A variety of SSEs, including organic polymer electrolytes (PEs), inorganic solid-state electrolytes (ISSEs) and PE and ISSE composites, have been investigated extensively^[11,12]. The fabrication of ideal SSEs should consider their mechanical strength, electrochemical window, chemical stability, cost and ionic conductivity. Generally, ISSEs can be classified into two categories: oxide solid electrolytes and sulfide solid electrolytes. PEs include solid polymer electrolytes (SPEs) and gel polymer electrolytes. Each type of SSE has its own relative merits. For example, ISSEs show higher ion conductivities at operating temperature, while PEs exhibit lower hardness, better interfacial contact and lighter weight. Thus, novel composite electrolytes may be enlightening in improving the performance of ASSLSBs because of their potential multifold benefits.

After decades of research, it is now clear that the main obstacle facing ASSLSB development is no longer improving the ionic conductivity of the SSEs but has instead shifted towards increasing the interfacial compatibility between the SSE and electrodes. The different interfacial nature of the electrode/SSE interface, in comparison with the electrode/liquid electrolyte interface, easily causes significant interfacial resistance^[13-16]. A good electrode/solid electrolyte interface should have excellent chemical and mechanical stability, high ion transport and maximum contact area during cycling. Currently, the electrode/electrolyte interface remains an important challenge that is limiting the possible commercialization of ASSLSBs. The resistance at the interfaces between the electrodes (anode and cathode) and SSEs is usually large. Favorable interfacial compatibility, contact and chemical stability are critical to improving the electrochemical properties of ASSLSBs [[Figure 1](#)].

Although a number of impactful reviews have summarized the progress and prospects of ASSLSBs, including SSEs, metallic lithium-based anodes and sulfur- and Li_2S -based cathodes, few reviews have specifically focused on the electrode/SSE interfaces in ASSLSBs^[18-23]. Therefore, to improve the understanding of the role of the solid/solid interfaces in these systems, this review provides a comprehensive summary and analysis based on the key interfacial challenges of electrode/SSE interfaces, including metallic lithium-based anodes/SSEs and sulfur- and Li_2S -based cathodes/SSEs, and SSE/SSE interfaces. The advanced strategies employed to resolve these interfacial issues are also introduced.

Evolution and classifications of ASSLSBs

Evolution

In order to understand the role of solid/solid interfaces in ASSLSBs, the evolution and classifications of

Table 1. Comparison of liquid electrolyte-based LSBs and ASSLSBs

| Batteries | Advantages | Disadvantages | Ref. |
|-------------------------------|---|--|--------|
| Liquid electrolyte-based LSBs | Higher conductivity Lower interfacial impedance | Polysulfide dissolution and shuttle Electrolyte decomposition Safety concerns (e.g., liquid leakage, inflammability and explosiveness) | [1,3] |
| ASSLSBs | Excellent thermal stability Nonflammable SSEs High operating voltages Low self-discharge Suppression of polysulfide dissolution Elimination of polysulfide shuttle | Poor interfacial stability Poor interfacial compatibility Large interfacial impedance | [7-10] |

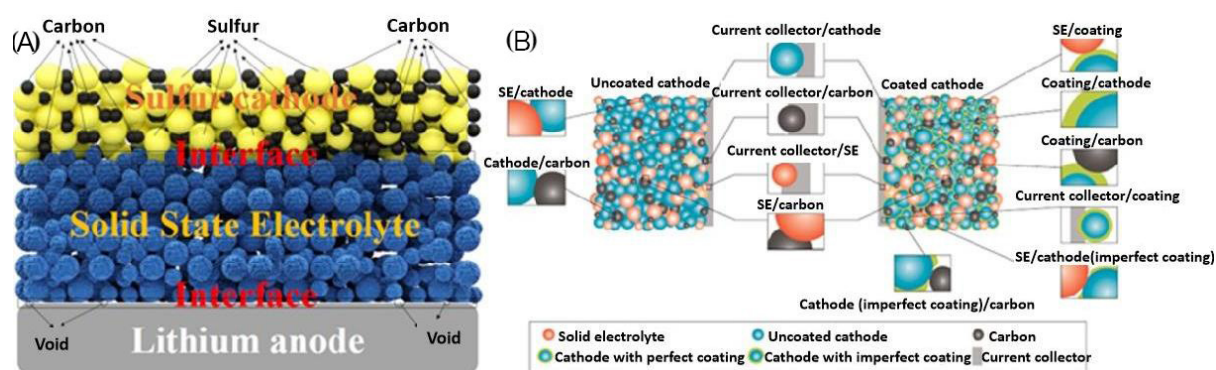


Figure 1. (A) Schematic illustration of interfacial compatibility and stability challenges in ASSLSBs. (B) Various interfaces in cathode composites (reproduced with permission from [17]).

ASSLSBs are briefly introduced here. The development of ASSLSBs has been accompanied by the study of fast lithium-ion conductors, such as $\text{Li}_2\text{S-P}_2\text{S}_5$ glasses, $\text{Li}_7\text{P}_3\text{S}_{11}$ glass-ceramics, solid polymer materials, thio-LISICON (Li superionic conductor, $\text{Li}_{4-x}\text{A}_{1-y}\text{B}_y\text{S}_4$ (A = Si or Ge; B=Zn, Al or Pt)), $\text{Li}_{10}\text{GeP}_2\text{S}_{12}$, argyrodites $\text{Li}_6\text{PS}_5\text{X}$ (X = Cl, Br or I) and composite polymer electrolytes, which have a history that can be traced back to the 1970s [24-26]. Following the discovery of SSEs with high ionic conductivities on the order of 10^{-3} - 10^{-2} S cm^{-1} , continuous efforts have been devoted to the fabrication of high-performance ASSLSBs. Currently, the Li-ion conductivity of LGPS-type $\text{Li}_{9.54}\text{Si}_{1.74}\text{P}_{1.44}\text{S}_{11.7}\text{Cl}_{0.3}$ is the highest (25 mS cm^{-1}) among all SSEs at room temperature [27,28], illustrating its potential application in ASSLSBs.

The number of publications dedicated to SSEs has increased dramatically since 2010, as shown in Figure 2A, indicating that they have become a research focus for energy storage with high power and density. The article search was limited from 1977 to December 2020 using Google Scholar. Of the 610 publications found [Figure 2B], 49.24% are focused on SSEs, suggesting that significant improvements have been achieved in their high Li-ion conductivities. The articles related to cathodes and anodes account for 16.75% and 11.68% of the total publications, respectively, aiming to resolve key issues in ASSLSBs, including volume change in the electrodes, low content or loading of active materials, insulating properties of S and Li_2S , chemical/electrochemical/physical instabilities, Li dendrite growth and side reactions between electrodes and SSEs. Only 3.21% and 5.75% of the publications investigate the mechanism and interfacial properties of ASSLSBs, respectively, showing that resolving the challenges at the electrode/electrolyte and electrolyte/electrolyte interfaces and revealing their mechanisms with advanced characterization tools remain significant challenges.

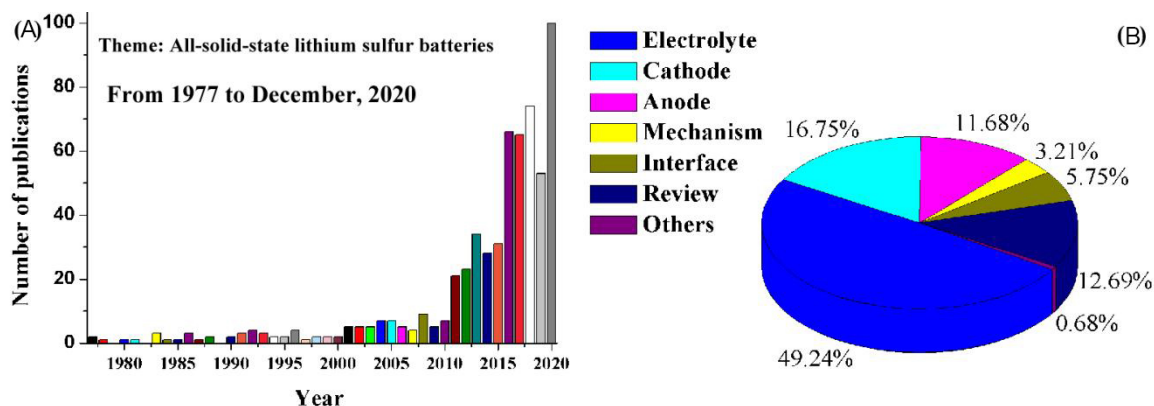


Figure 2. (A) Approximate publication numbers of ASSLSBs per year (from 1977 to 2020) and (B) a comparison of themes addressed in the literature.

Classifications

A variety of active materials and SSEs have been applied to fabricate ASSLSB systems. According to the topic and electrolyte, cathode and anode types, ASSLSBs can be approximately classified into 11 categories, namely, sulfur, Li_2S , metal sulfide, Li alloy, Li-inorganic material composite, glass, glass-ceramic, argyrodite, thio-LISICON, LiBH_4 and composite electrolyte based, as shown in Figure 3. The disadvantages and advantages of the various types of ASSLSB systems are summarized in Table 2.

Cathodes

A number of cathode materials have been investigated so far and three main cathode materials, namely, sulfur-, Li_2S - and metal sulfide-based cathodes (e.g., Co_9S_8 , FeS_x , CuS , MoS_3 and SeS_x), have been proposed for ASSLSBs [Figure 4]^[31,41-46]. To achieve high performance, a cathode material must satisfy several conditions, including small volume changes, high electronic and ionic conductivity, low cost, environmentally friendly, high theoretical capacity, good thermodynamic stability, high stability against SSEs and good interfacial compatibility with SSEs^[47-52]. The ideal cathode designs for high-performance ASSLSB systems are more complicated. The development of composite materials consisting of the active material, Li^+ ion conductor and electronic conductor by combining their advantages could be a good alternative, but their properties are seriously affected by the particle size, host construction and types and mixing methods of the cathode materials. Further enhancements in the interfacial compatibility of cathodes with SSEs, especially maintaining their interfacial stability, are very important for the practical applications of ASSLSBs.

Anodes

The use of Li metal anodes is very attractive and a key target for ASSLSBs due to the relatively low redox potential (-3.040 V vs. a standard hydrogen electrode) and high theoretical capacity (3860 mAh g^{-1}) of Li metal. However, continuous Li dendrite growth, large volume changes, low operation current and unstable Li metal/SSE interfaces during cycling hinder the practical applications of Li metal anodes. To address these issues, the Li-M alloys ($M = \text{In, Sn, Ge, Cu, Ni, Hg, Ag, Au, Mg}$ or Al)^[53-62] and Li-inorganic material (e.g., C, Si, oxides, nitrides or sulfides) composites have been developed^[63-68]. These strategies not only effectively approve the interfacial contacts of anodes with the SSEs but also increase their chemical and electrochemical stability and block their side reactions with the SSEs, further enhancing the sluggish reactions at the interface and suppressing the Li dendrite formation because of the strong bulk modulus and the high interfacial energy^[32,69-73]. Their mechanical properties, chemical stability and electrochemical stability should

Table 2. A summary of the advantages and disadvantages of various ASSLSB architectures

| Cathode | Anode | Electrolyte | Advantages | Disadvantages | Ref. |
|-------------------|----------------------------------|--|---|--|------|
| Sulfur | - | - | Earth-abundant, low cost, environmentally friendly and a high theoretical specific capacity | Low cathode utilization, low active loading in cathode composites, huge volume change, low electrochemical kinetics and highly insulative | [29] |
| Li ₂ S | - | - | Stable cycling life, excellent capacity retention and high discharge capacity | Highly insulative and low theoretical specific capacity and matching with lithium-free anode materials | [30] |
| Metal sulfides | - | - | Improved interfacial electronic conductivity, long cyclic life and good interfacial contact of active material/electrolyte | Low theoretical capacities, low discharge voltages and large volume change | [31] |
| - | Li alloys | - | High stability in ambient air, improving the Li/SSE interface contact, improving the sluggish Li ⁺ transport, realizing dendrite-free Li deposition and small volume changes | Increased costs, compromised overall specific capacity and higher operating potentials | [32] |
| - | Li-inorganic material composites | - | Enhancing the structural stability, suppressing the lithium dendrite growth, blocking its side reactions, high interfacial energy and high bulk modulus | Poor cycle life and rate capabilities, parasitic interfacial reactions and higher operating potentials | [33] |
| - | - | Glass Li ₂ S-P ₂ S ₅ | Good mechanical strength and flexibility and low grain boundary resistance | Low oxidation stability, sensitivity to moisture, poor compatibility with cathode materials, low ionic conductivities at room temperature and narrow voltage windows | [34] |
| - | - | Glass-ceramic Li ₇ P ₃ S ₁₁ | High conductivity, low grain boundary resistance, inherent isotropic character and sufficient plasticity | Hygroscopic, low oxidation stability and limited voltage windows | [35] |
| - | - | Thio-LISICON Li ₁₀ GeP ₂ S ₁₂ Li ₁₀ SnP ₂ S ₁₂ | High bulk conductivity, good thermal stability and outstanding mechanical strength | Poor stability against Li metal anodes, narrow electrochemical stability windows, high interfacial impedance and degraded physical stability with electrodes | [36] |
| - | - | Argyrodite Li ₆ PS ₅ X (X = Cl, Br or I) | Low-cost precursors and wide electrochemical window | Unstable with polar organic solvents and low ionic conductivities at room temperature | [37] |
| - | - | LiBH ₄ | Superior chemical/electrochemical stability against Li metal | Low room-temperature ionic conductivity | [38] |
| - | - | Polymer | Stable with lithium metal, flexible, easy to produce a large-area membrane, low shear modulus and low interfacial impedance | Limited thermal stability, low ionic conductivities at room temperature and narrow electrochemical stability windows | [39] |
| - | - | Polymer-based composites | Low interfacial impedance, high ionic conductivity and balancing the merits and drawbacks of each component | Low mechanical strength and poor thermal stability | [40] |

be considered for the improvement of the interfacial compatibility of anodes with SSEs, as the anodes are properly designed. However, the relatively higher operating potentials of the modified Li anodes inevitably result in a decreased energy density. An in-depth understanding of the fundamentals and engineering principles of Li/SSE interfaces is an underlying challenge for ASSLSBs.

Electrolytes

SSEs are a family of solid-state ionic materials (also known as fast ion conductors or superionic solids) that exhibit remarkable technological potential for designing safe and high-performance all-solid-state electrochemical energy storage systems, because of their extremely high room temperature ionic

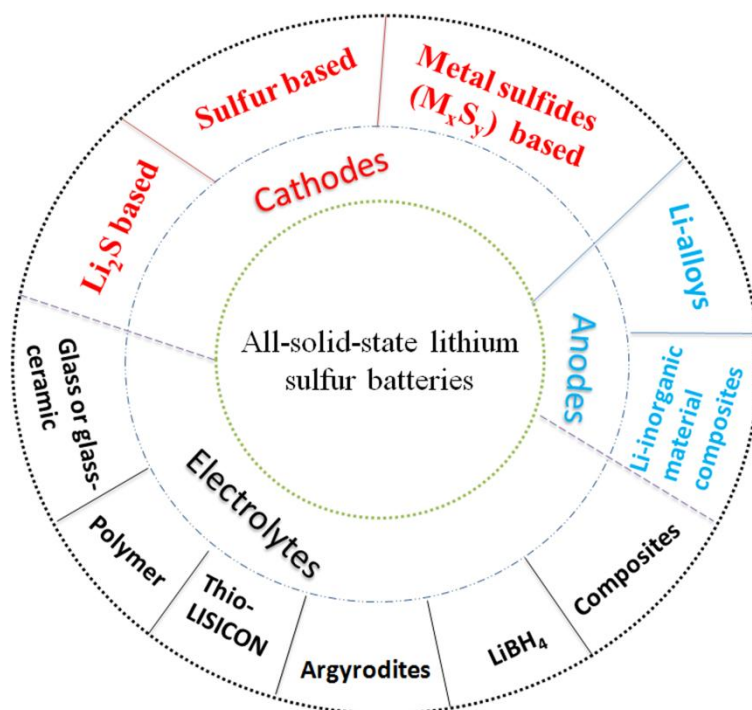


Figure 3. A summary of the various types of cathodes, anodes and electrolytes used in ASSLSBs.

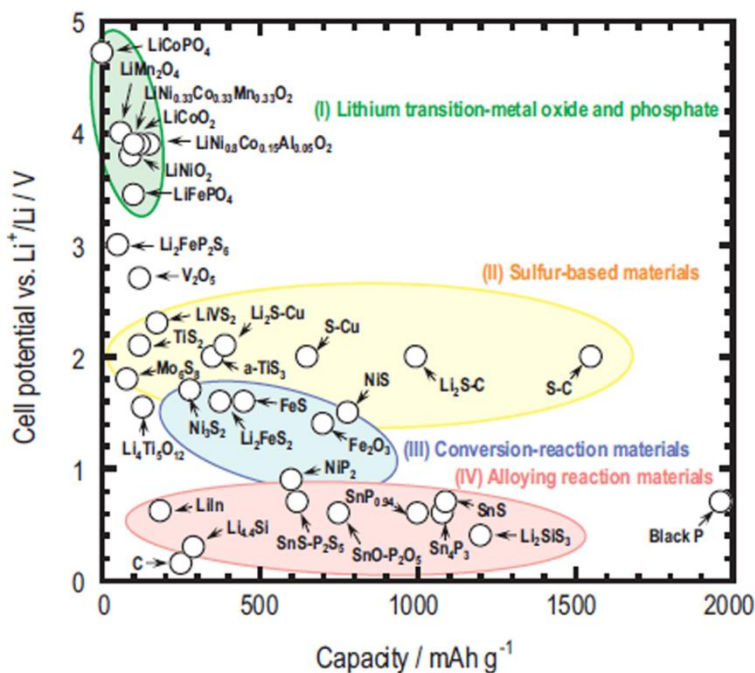


Figure 4. Comparison of various cathode materials employed in ASSLSBs with a sulfide SSE (reproduced with permission from^[46]).

conduction (close to or even higher than that in the range of liquid electrolytes). Although ionic conductivity is a critical characteristic for SSEs, other features are also vital to their practical application, such as mechanical properties, ionic selectivity, electrochemical stability window, thermal stabilities, cost,

construction processes and methods, chemical compatibility and non-poisonous. Several kinds of SSEs have been designed and prepared, including inorganic SSEs (in the three major categories of sulfides (e.g., glass and glass-ceramic $\text{Li}_2\text{S-P}_2\text{S}_5$, argyrodite and thio-LISICON), oxides and LiBH_4), organic (polymer) SSEs and hybrid electrolytes^[74-78]. However, most SSEs suffer from volume changes and large interfacial impedances during cycling. In composite systems, inorganic SSEs are expected to be organically combined with organic SSEs to take advantage of each single-component SSE and reduce their drawbacks. Nevertheless, it is still difficult to design and develop ideal electrolytes with many advanced properties, including high ionic conductivity, good mechanical properties, a wide electrochemical window and excellent thermal and chemical stability.

In most cases, solid sulfur and its composites serve as the cathode for ASSLSBs, which is directly reduced to form Li_2S at the plateau of ~ 2 V during discharge and the dissolution of polysulfides cannot occur because of the employment of SSEs. In the presence of composite electrolytes with a small part of polymer or liquid electrolytes, the formation and dissolution of intermediate polysulfides can occur at the beginning of discharge. The two different types of the electrochemical reaction mechanism of ASSLSBs, a solid-solid single-phase reaction and a solid-liquid dual-phase reaction, inevitably result in unique opportunities and new challenges for the design and fabrication of electrode and electrolyte materials.

To summarize this section, for the components of ASSLSBs, mainly including anodes, cathodes and electrolytes, besides their theoretical specific capacity and conductivity, the thermal, structural, chemical and electrochemical stability, mechanical strength and synthesis method are also critical factors affecting the comprehensive properties of ASSLSBs. The current operating electrochemical performance of ASSLSBs is generally unsatisfactory. The poor interfacial compatibility between the electrode and electrolyte is still the major bottleneck for the development of high-performance ASSLSBs.

Brief overview of issues related to ASSLSBs

Since most of the components in ASSLSBs are solid particles, ASSLSBs are usually assembled by directly stacking the anode/electrolyte/cathode cell components in a single package, unavoidably leading to the formation of many interfaces between particles (e.g., anode/electrolyte, cathode/electrolyte, electrolyte/electrolyte and additive/electrolyte interfaces) [Figures 1 and 5]. Unlike liquid electrolyte-based LSBs, the nature of the solid/solid interfaces in ASSLSBs can cause serious interfacial issues:

- (a) The poor interfacial contact originating from the stress/strain at the SSE/cathode interface induced by the volume change of active materials, such as Li_2S or S, during cycling leads to high interfacial impedance.
- (b) Several kinds of anode/SSE interfacial issues, including the electrochemical instability of SSEs against metal lithium, Li dendrite penetration and poor interfacial compatibility, contribute to degrading the performance of ASSLSBs.
- (c) The interphase between an electrode (cathode or anode) and electrolyte induced by redox instability of the SSE results in low Li^+ interstitial conductivity.
- (d) The electrochemical instability of sulfide-based SSEs against ambient air causes the generation of harmful by-products. Furthermore, most of these by-products have limited voltage windows and can be unstable (oxidized at high voltages or reduced at low voltages) at the full voltage range of the electrode materials, contributing to the formation of interphases.

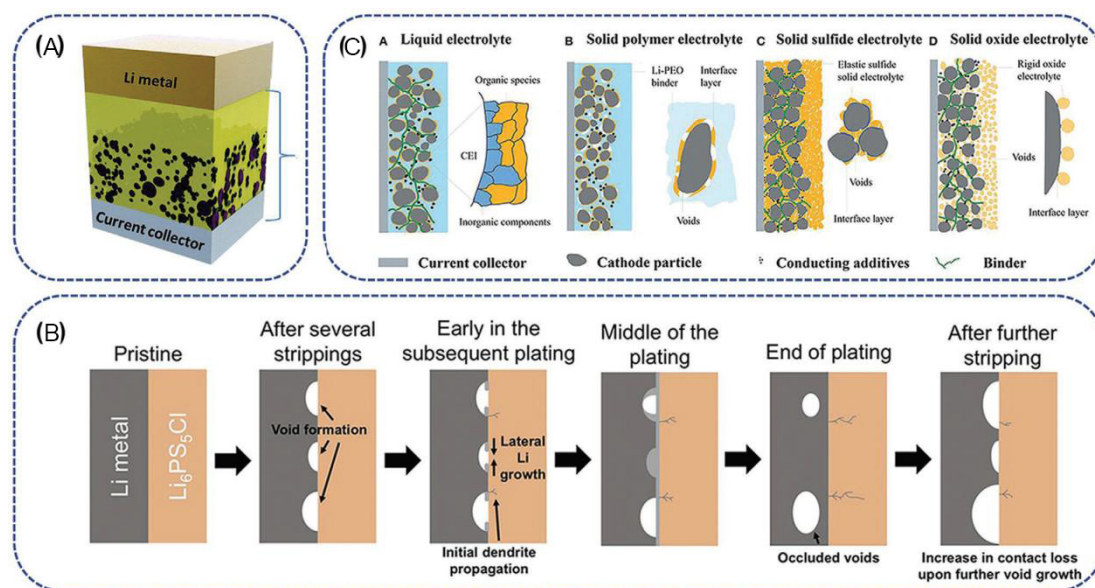


Figure 5. (A) Schematic illustration of solid-state lithium cell (reproduced with permission from^[7]). (B) Evolution of anode interface at different stages (reproduced with permission from^[8]). (C) Interface models of three representative SSEs (reproduced with permission from^[9,10]).

(e) Grain boundary resistance induced by the space charge and interphase layers generally exists at solid/solid interfaces.

(f) Voids resulting from the packing technology of cells and electrode pulverization and Li metal dendritic growth increase the interfacial resistance.

(g) The low active loading in cathode composites, low cathode utilization and low ionic/electronic conductivity of S and Li_2S result in unsatisfactory capacity output.

(h) An understanding of the interfacial kinetics, electrochemical reactivity and microstructure of interfaces remains a challenge for ASSLSBs.

(i) Transforming laboratory cells into real commercial ASSLSB products remains an additional hurdle.

In the following section, in order to further understand the interfacial issues mentioned above, a detailed discussion of the possible cause of the formation of the interface is presented.

ORIGIN OF ELECTRODE/SSE INTERFACE

The interfacial issues of ASSLSBs are always present at both the anode and cathode sides. The interface can be defined as a surface forming a common boundary between the adjacent regions of the electrode and SSEs^[35,79]. The corresponding interfacial resistance is a key factor affecting the performance of ASSLSBs, which is related to interfacial contact condition, ion transport, chemical potential differences, interfacial energy and structural stability. Multiple physical and chemical processes often occur at interfaces during cycling, including mutual diffusion, ionic transport, a lithium-depleted space-charge layer, solid electrolyte interface formation and decomposition, dendrite growth and electrode volume expansion, which could be the main cause of the formation of the interfaces between electrodes and electrolytes^[35].

Anode side

Employing lithium metal as the anode in an ASSLSB configuration can result in 70% and 40% improvements in the gravimetric and volumetric energy density, respectively; however, unstable Li metal anode/SSE interfaces caused by the poor contact and side reactions during cycling potentially give rise to high interfacial resistance, capacity fading and battery failure.

Poor interfacial contact

In comparison with liquid electrolytes, owing to the intrinsic rigidity and relatively high stability of SSEs against Li metal and their mismatched lattice, SSEs cannot easily wet the electrode surface and only point-to-point contacts between the lithium metal anode and SSEs can be achieved, resulting in the interfacial voids and defects, dendrite growth of Li along the grain boundaries and a loss of interfacial contact^[10]. Furthermore, significant volume changes between the anode and SSEs during cycling trigger the interfacial stress changes, leading to poor physical contact and an increase in interfacial resistance, which is unfavorable for lithium ion transfer. In comparison with ISSEs, SPEs show higher interfacial compatibility with lithium metal anodes, but their low ionic conductivity greatly restricts their application in ASSLSBs.

Chemical reactions

In addition to poor contact, side reactions at the Li metal anode/SSE interface can lead to an increase in interfacial resistance. Since Li metal anodes have an ultralow electrochemical potential, they can directly react with various kinds of SSEs during the packing process. In addition, the Li metal anode and electrolytes can offer a high thermodynamic driving force for electrochemical oxidation and chemical reaction to form interfacial regions during cycling^[7,80] [Figures 6 and 7].

The resistance of the formed interface is determined by the chemical composition of the interphases. For example, harmful by-products, such as Li ionically/electronically insulating $\text{Li}_2\text{S}/\text{LiX}$ ($\text{X} = \text{Cl}, \text{Br}$ or I) produced by the interfacial reactions of Li metal with sulfide solid electrolytes, contribute to the increase in the interfacial resistance. According to the thermodynamical stability of the interface, three different types of interface formation are proposed [Figure 7A-C]^[81]. An interface that is electronically insulating and ionically conductive could possess high electrochemical stability during cycling, while thermodynamically unstable interfaces with mixed ionic-electronic conducting interphases keep growing. The Li ionic conductivity of the interface is very important for the performance of ASSLSBs.

Furthermore, the interphase layer between the Li metal anode and electrolyte arises from the redox instability of the SSEs. Both a reasonable alignment of the electrolyte bands, including the valence and conduction bands, relative to the Li chemical potential μ_{Li} , and a relatively high band gap are two critical factors affecting the redox stability of the SSEs.

The values of the electrochemical stability window can be obtained by first-principles calculations and experimental measurements [Figure 7D]^[82]. As a result, the calculations predict that sulfide SSEs can only afford a narrow voltage stability window, while Li binaries, Li_nX ($n = 1, 2$ or 3 ; $\text{X} = \text{anion}$), exhibit an expected trend of extending voltage stability window with increasing anion electronegativity.

Although the formed interphase layer can inhibit dendrite growth, a continuous decomposition and interphase layer growth are usually contributed by the electron transfer across this mixed interphase layer, severely increasing the local volume, polarization and interfacial impedance during the cycle. Additionally, the volumetric expansion can also result in repeated cracking and finally damage the SSE.

potential, conductivity, mechanical properties (e.g., Young's and shear moduli), thermal stability, defect density and the concentration of elements/charge carriers are the key determinants of interface formation^[45,83-85]. The electrochemical processes mainly occur at the multi-phase interface of the solid components in the composite cathode during cycling. The formed interfaces between the cathode and electrolyte differ from an interface of active materials/electronic conductors to an interface of active materials/Li-ion conductors. A number of issues may simultaneously coexist at the cathode/electrolyte interface, including incomplete interfacial contact, interfacial decomposition, space-charge layers, polarization and chemical interdiffusion, which are regarded as the major reasons for the increased interfacial resistance.

Volume changes

Generally, a significant volume change (up to ~80%) occurs between the sulfur and Li₂S during battery cycling; thus, regardless of the type of SSE, the cathode/SSE interfaces normally suffer from contact failure. In the case of cathode composites, the volume ratio and geometric arrangement between different solid components are critical factors that affect the volume change, thereby determining the structural stability of the cathodes.

Interfacial reactions

Cathode composite systems consisting of several components contain multi-interfaces and spontaneously evolve towards a nonequilibrium thermodynamic state and a chemical potential gradient exists across the interfacial interactions because, in most cases, the electrochemical windows of SSEs cannot adequately match the chemical potential of cathode (μ_c) materials^[86,87]. The electrochemical windows of SSEs are completely dependent on the energy separation E_g between the conduction band or lowest unoccupied molecular orbital (LUMO) and valence band or highest occupied molecular orbital (HOMO) [Figure 8]. The thermodynamic stability of an interface is strongly determined by the Fermi energy of the electrodes. If μ_c (μ_c for cathode) is below the HOMO of the SSEs or μ_a (μ_a for anode) > LUMO, the interface is thermodynamically unstable. The nonequilibrium thermodynamic state can provide a thermodynamic driving force at an interface, causing the interfacial reactions between the two components to form the cathode/electrolyte interphases.

In comparison with oxide cathodes, sulfide-based cathodes exhibit more intimate interfacial contact and similar chemical potentials with sulfide electrolytes; thus, the key issue increasing the cathode/electrolyte interfacial resistance could be the stress/strain induced because of the volume change of the sulfide cathodes. However, it has been found that the chemical interaction and interfacial decomposition that simultaneously occur at the interface may be non-negligible disadvantages that restrict the stability of cathode/electrolyte interfaces. SSEs have limited thermal stability during high temperature or pressure processing and weak electrochemical stability during cycling, with the induced formation of an interphase resulting from nonequilibrium side reactions controlled by the kinetic process. In addition, the interfacial reactions between sulfide-based SSEs and sulfur are also observed and form undesired insulating by-products, which can be attributed to the reaction of the functional groups with sulfur. As a result, the undesired insulating by-products caused by the side interfacial reactions are detrimental to the interfacial ion conductivity.

In spite of tremendous efforts to investigate the interfaces between solid electrolytes and electrodes, a comprehensive understanding of their role has not yet been achieved. A deep understanding of these complex interfaces, including the formation mechanisms of the interphase, components, microstructures, pathways of Li-ion diffusion and dynamic characteristics, is crucial to developing future ASSLSBs. The

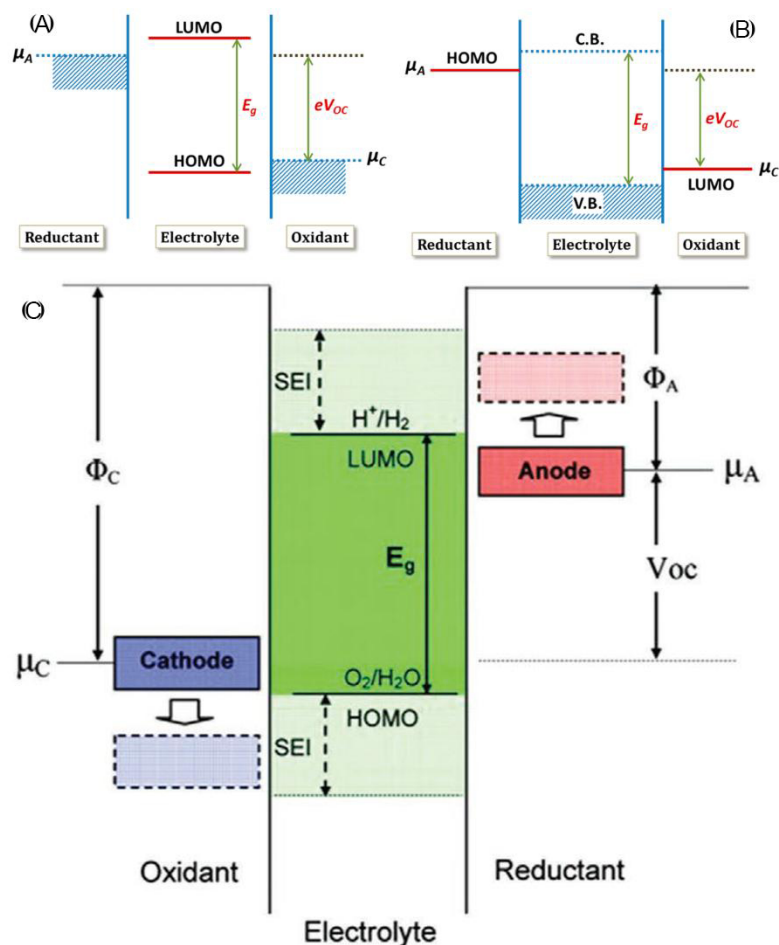


Figure 8. Open-circuit energy diagrams of various cell systems. (A) Overall illustration of a cell consisting of a liquid electrolyte (μ_c and μ_a represent the energy levels of the cathode and anode materials, respectively, HOMO and LUMO refer to the highest occupied and lowest unoccupied molecular orbitals of the liquid electrolyte, respectively, C.B. and V.B. represent the conduction and valence bands of the SSE, respectively, and V_{oc} represents the open-circuit voltage of the cell). (B) Stable energy window related to liquid electrolyte and (C) SSE (reproduced with permission from [87,88]).

investigation and understanding of the interfaces in ASSLSBs require computational methods to effectively predict and reveal the interfacial stability properties because most direct experimental detecting techniques easily destroy the solid/solid interfaces in the separation process of samples.

COMPUTATIONAL PREDICTION OF INTERFACIAL STABILITY BETWEEN ELECTRODES AND SSES

Owing to their high-throughput nature, several computational methods, including density functional theory and ab initio molecular dynamics simulations, have been employed to identify the theoretical/intrinsic formation of interfaces, confirm the existence of space-charge layers and analyze the possible interfacial reactions in a working cell. The stability of electrode/electrolyte interfaces at various levels can be evaluated systematically [89–92].

Cathode side

For both conventional liquid electrolyte-based LSBs and ASSLSBs, conductive host materials are an integral part of S-based cathodes due to the insulating nature of S and lithium sulfide. In various types of host

materials, carbon-based groups afford relatively strong affinity for polar LiS species (calculated binding energy of 0.30 eV); however, an electron source from carbon can accelerate the electrochemical decomposition of sulfide-based SSEs, contributing to the formation of the cathode/electrolyte interface.

Computational studies can also be used to predict the electrochemical window of SSEs, as in the previous sections, which is normally less than the redox potential of cathode active materials, indicating that most SSEs show high instability in contact with cathodes during cycling. For sulfide SSEs, the calculated oxidation potential is $\sim 2.15\text{--}2.31$ V^[90] and a series of the decomposed interfacial products can be computationally confirmed (e.g., S, P₂S₅, Li₄P₂S₆ and Li₂S for Li₃PS₄ and Li₃PS₄, GeS₂, S, Li₄GeS₄, Li₄P₂S₆ and Li₂S for LGPS).

Although the interfaces between sulfide-based cathodes and SSEs could be very stable compared to oxide cathodes because sulfide-based cathodes show similar chemical potential with sulfide-based SSEs, their interface with limited ionic conductivity cannot be favorable for the development of ASSLSBs with high electrochemical performance. In order to further understand the interface stability of sulfide-based cathodes/SSEs, the prediction of their thermodynamic reaction energy, the exact reaction pathway and possible interfacial reactions using theoretical calculations should be performed, the existence of a space-charge layer confirmed and the interface modeled.

Lithium metal anode side

It has been found that theoretical calculations are very efficient and powerful tools for investigating and analyzing the properties of anode/SSE interfaces and interfacial evolution behavior of ASSLSBs during cycling, significantly contributing to understanding the role of interfaces in ASSLSBs. The Li metal anode shows a high adhesion (W_{ad}) predicted by density functional theory calculations when exposed to SSEs, which can be used to reveal the possible working mechanism of the interfacial layer between the anode and electrolyte^[93]. Furthermore, a series of interfacial reactions between anodes and electrolytes can be predicted by theoretical calculations. The results show that sulfide-based SSEs, including Li₃PS₄, Li₇P₃S₁₁, Li₇P₂S₈I, Li₆PS₅Cl and LGPS, have low thermodynamic stability against Li metal, are usually reduced during assembling and cycling and possibly form Li-based interfacial products, such as Li₂S, Li₃P, Li-metal alloys, LiCl and LiI.

Computational studies are also used to reveal the mechanical properties of the Li metal/SSE interface, such as Young's, bulk and shear moduli and estimate their effect on the formation and growth of Li dendrites at the anode/SSE interface. The result indicates that Li dendrite propagation in the SSE should be suppressed if the shear modulus of an electrolyte is higher than twice that of Li metal.

Ultimately, theoretical calculations, combined with experimental characterization methods, including scanning tunneling microscopy, scanning transmission electron microscopy (TEM), X-ray diffraction (XRD), X-ray photoelectron spectroscopy (XPS), infrared and Raman spectroscopy, nuclear magnetic resonance spectroscopy, X-ray absorption spectroscopy and binding energy, can be the most efficient route to exploring the interfacial properties between electrodes and electrolytes, analyzing their interfacial resistance, predicting the structural and chemical information of the interface and providing essential guidelines for screening and designing stable interfaces.

CURRENT KEY CHALLENGES OF SOLID/SOLID INTERFACES BETWEEN ELECTRODES AND SSES

As discussed earlier, the major issues result from the interfaces between SSEs and electrodes in typical ASSLSBs. Various kinds of SSEs have been applied to ASSLSBs, including organic polymers, inorganic materials and organic-inorganic hybrids, and their reactivity with electrodes contributes considerably to the internal resistance of the battery. Several parameters or properties of an electrolyte play a critical role in determining the performance of interfaces, namely, ionic conductivity, interfacial properties, mechanical properties, electrochemical stability and compatibility with the electrodes during battery cycling tests [Figure 9]^[94-97]. ASSLSBs employing different SSEs could face different interfacial challenges because of their different electrochemical reaction mechanisms at the electrode/SSE interfaces.

Issues facing cathode/electrolyte interfaces

The cathode materials in ASSLSBs have been intensively reported. The cathode/electrolyte interfacial issues induced by the electrochemical potential occur during cycling and are significantly different for various electrolytes. However, owing to the low operation potential (< 2.8 V vs. Li/Li⁺) of sulfur-based cathodes, their interfacial electrochemical reaction is negligible for SSEs. Therefore, the main concern at the cathode sides of ASSLSBs could be the chemical stability of SSEs in contact with cathodes (S or Li₂S based)^[98-101]. The following sections summarize and discuss the relationship between interfacial issues and categories and the interfacial reactions and interphase formation between the cathode and electrolyte.

Cathode/organic polymer electrolytes

SSPEs possess several special advantages, including good interfacial compatibility, high safety, easy preparation, flexibility, lightweight and the possibility of scalable roll-to-roll manufacturing processes, and they have been considered as promising candidates for the development of safe ASSLSBs. However, several issues hinder the development of SSPEs in ASSLSBs, such as low room-temperature ionic conductivity and poor thermal stability. In particular, a high diffusion of lithium polysulfides in the organic matrixes often fails to inhibit their formation and shuttle and a S-rich passivation layer on the Li metal anode surface could be formed and observed after cycling^[102]. In order to block the polysulfide dissolution and shuttle for high-performance solid-state polymer-based ASSLSBs, S-based composite electrode materials combined with SSPEs have been proposed, as presented in the following sections.

Cathode/inorganic SSEs

Inorganic SSEs can be further classified as oxide or sulfide-based SSEs. Although remarkable progress in the development of oxide SSEs has been made, there remains a challenge to adequately integrate oxide SSEs, including perovskite-type Li_{1-3x}La_{(2/3)x}TiO₃ (LLTO), garnet-type Li₂La₃Zr₂O₁₂ (LLZO), NASICON-type Li_{1+x}Al_xTi_{2x}(PO₄)₃ (LATP) and Li_{1+x}Al_xGe_{2x}(PO₄)₃ (LAGP), into ASSLSBs because of the obvious differences between the thermal and chemical properties of oxide SSEs and S-based cathodes, the poor interfacial compatibility and large grain boundary resistance^[4,13,15,20].

In addition to oxide SSEs, sulfide-based SSEs with high room-temperature ionic conductivities of 10⁻² S cm⁻¹ have also been considered in the design of favorable SSEs for inorganic SSE-based ASSLSBs, such as glass sulfide, glass-ceramic and crystalline sulfide SSEs. Compared with oxide SSEs, sulfide-based SSEs exhibit low grain boundary resistance; however, several major shortcomings of the single-component sulfide-based SSEs still limit their application in ASSLSBs, including high chemical instability against moisture and narrow electrochemical stability windows (in the range of 1.5-2.5 V). Normally, inorganic SSEs are coupled with liquid electrolytes, ionic liquids or polymer-based SSEs for the improvement of their interfacial behavior.

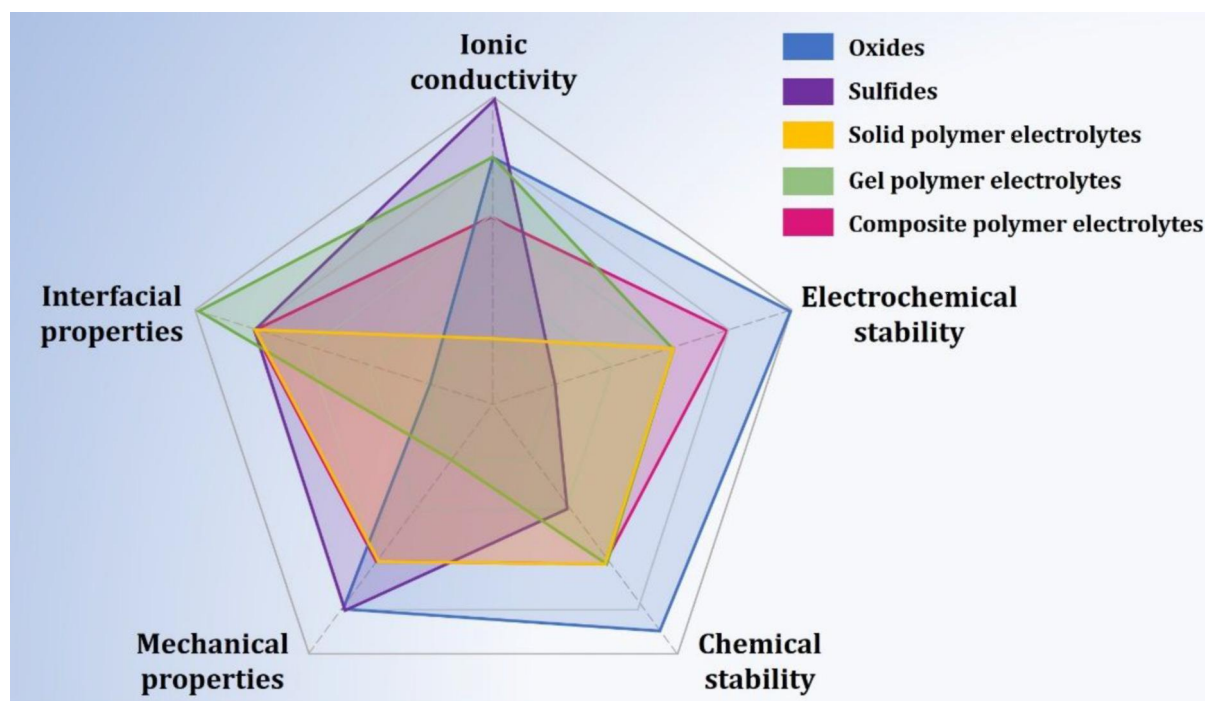


Figure 9. Radar charts of various SSEs, including gel polymers, sulfides, solid polymers, oxides and composites to compare their performance (reproduced with permission from^[97]).

Cathode/hybrid electrolytes

In order to improve the interfacial properties, ionic conductivity and mechanical, thermal, chemical and electrochemical stabilities of single-component SSEs, a new strategy of hybrid SSEs has been proposed by rationally configuring different types of SSEs to mitigate the drawbacks of each component. The addition of inorganic material additives to the organic polymer matrix leads to the enhancement of the electrolyte/cathode interfacial performance^[9,21,23,45,103,104]. Benefitting from the merits of inorganic SSEs (e.g., high mechanical strength and ionic conductivity) and soft components (such as good interfacial compatibility), the issues at cathode/SSE interfaces and the polysulfide shuttle problem are significantly relieved, which could be attributed to the formation of Li^+ -filler complexes. Therefore, composite electrolytes composed of flexible components and stiff inorganic materials additives have more application potential.

Issues facing anode/electrolyte interfaces

In this section, the behavior of Li metal anode/SSE interfaces during cycling is discussed. It is clear that direct contact between a Li metal anode and SSEs can result in the formation of a series of reduction products at the interface, resulting in interfacial issues. The chemical compositions of the interphases formed at the interface between anodes and SSEs and their interfacial properties are determined by different cation chemistries. For example, the formed side-products for LLZO at the anode/electrode interface mainly include Li_8ZrO_6 , Zr_3O , Zr , La_2O_3 and Li_2O after contact with lithium, while for solid polymer electrolytes, LiF and lithium alkoxide^[105], phosphorus oxynitride, Li_3P , Li_3N , and Li_2O , and for perovskites, La_2O_3 , Li_2O and metallic Ti_6O ^[90], generally increasing the interfacial resistance of the anode/electrolyte interface. Furthermore, Li dendrite formation and growth and the poor interfacial stability between the Li metal anode and SSEs during cycling are also major barriers to the development of practical ASSLSBs. Further research is still therefore required.

Anode/organic polymer electrolytes

Owing to their poor mechanical strength, Li dendrite growth is still a serious issue for SPEs in the realization of ASSLSBs, easily causing the internal short circuits of cells. To overcome this problem, various kinds of inorganic filler, including sulfides and oxides, have been introduced into the SPEs to improve their mechanical properties, as well as ion conductivities in ASSLSBs, which is believed to be one of the ultimate choices for suppressing Li dendrite growth and blocking the shuttling of lithium polysulfides^[22,64,106-108].

Anode/inorganic SSEs

Furthermore, different interfacial properties can be observed in the interphases of Li metal anode/inorganic SSEs, which are demonstrated to be associated with their thickness. For example, a 20 μm interphase layer containing Li-Ti/Ge alloys is found at a NASICON-type electrolyte/Li metal anode interface^[109]. A passive layer with a thickness of 2 nm, consisting of Li_2S species, is formed at the anode/electrolyte interface after Li metal contact with sulfide electrolytes^[110]. Such unstable interphase layers that often block the interfacial ionic transport eventually lead to increased interfacial resistance. Furthermore, Li dendrite formation in sulfide electrolytes seriously hinders the development of safe ASSLSBs.

In contrast, a few oxide SSEs, particularly LLZO, exhibit high chemical stability against the Li metal anode and the resulting passivation layer has the ability to conduct Li ions (e.g., Li_2O , Zr_3O and La_2O_3) to restrain the continuous degradation of the SSE/Li metal interface^[13,111-114]. However, unlike liquid electrolytes, most have poor wettability with the Li metal anode because of their rigid and brittle nature, resulting in the loss of intimate contact and high interfacial resistance between the Li anode and oxide SSEs.

Anode/hybrid electrolytes

Compared to single-component electrolytes (solid-state inorganic electrolyte or solid-state polymer), the interfacial behavior of polymer-inorganic composite electrolytes, including interfacial compatibility, chemical stability, safety and mechanical strength, can be effectively improved and the polysulfide shuttle and Li dendrite growth are suppressed. The interfacial properties of a Li anode/polymer-inorganic composite electrolyte depend not only on the spatial distribution of each species but also on their own stability. However, the room-temperature ionic conductivity of polymer-inorganic composite electrolytes is still low and their interfacial stability against Li metal anodes is very complicated. The following section presents a detailed discussion of the possible strategies and selection criteria to mitigate these issues for the development of high-performance ASSLSBs.

STRATEGIES FOR RESOLVING INTERFACIAL ISSUES

Current ASSLSBs still show lower cycle life and rate capability than liquid batteries because of the previously discussed SSE/electrode interfacial issues. In order to solve these interfacial issues and improve battery performance, various significant strategies have been conducted, including interfacial engineering, adding ionic conductive materials, the application of artificial coating layers, reducing the active material particle size, employing a hot- or cold-press setup, the utilization of fillers and designing composite cathodes.

Sulfur cathode side

Pure sulfur-based active materials have poor ionic and electronic conductivity, usually leading to high interfacial resistance and poor battery performance. In order to improve their ionic and electronic conductivity, large amounts of SSE and electronic conductors need to be added to the composite cathodes separately. Designing and fabricating composite cathode materials composed of active materials (e.g., sulfur and sulfur-based constituents), Li-ion conductors (e.g., SSEs), electronic conductors (e.g., carbon and metal) and/or binders have been demonstrated to be effective strategies for improving the ionic and electronic

conductivity of cathodes, increasing the contact area at the cathode/SSE interface and decreasing the interfacial resistance. However, the conductivity of sulfur-based electrodes could not be significantly enhanced by simply mixing carbon and SSEs with sulfur. The low interfacial resistance seriously depends on the component and preparation method of composite cathode materials [Figure 10 and Table 3].

Constructing composites consisting of Li-ion conductors, electronic conductors and sulfur-based active materials

Ball milling is a technique that can provide the mechanical energy to break the order of a crystalline structure, decrease the particle size of electrode materials, prepare an intimate contact and generate a favorable interface between the active material, conducting additive and Li-ion conductor. Therefore, ball milling has intensively been employed to prepare various sulfur-based cathode composites of ASSLSBs, including S/Cu₂S/acetylene black (AB)/80Li₂S/20P₂S₅^[120], sulfur/poly(ethylene oxide) (PEO)/AB^[121], S/carbon/PEO/acetonitrile^[122], S/AB/thio-LISICON (Li_{3.25}Ge_{0.25}P_{0.75}S₄)^[123], Li₂S/80Li₂S/20P₂S₅/Cu^[124], 80Li₂S/20P₂S₅-Cu^[125], S/AB/80Li₂S/20P₂S₅^[149], Li₂S/AB/80Li₂S/20P₂S₅^[127], S/graphite^[128], sulfur/carbon/thio-LISICON^[129], vapor-grown carbon fiber (VGCF)/S/ionic liquid/ α -Li₃PS₄^[130], sulfur/activated carbon/P₂S₅^[131], sulfur/super P carbon/Li₆PS₅Br^[132], sulfur/AB/75Li₂S·25P₂S₅^[116], S-C/Li₆PS₅Cl/super P^[133], S/C/Li₇P_{2.9}Mn_{0.1}S_{10.7}I_{0.3}^[116], S-graphene oxide/Li_{9.54}Si_{1.74}P_{1.44}Cl_{0.3}/carbon black^[99], Li₂S-VGCF/78Li₂S·22P₂S₅/Ketchen black conductive carbon^[83], reduced graphene oxide-S/Li₁₀GeP₂S₁₂/AB^[84], S/AB/70Li₂S·30P₂S₅^[134], Li₂S/super P carbon/VGCF/70Li₂S·30P₂S₅^[137], S-C-FeS₂/Li₃PS₄-LiI^[150], S-carbon nanotubes/multi-wall carbon nanotubes/78Li₂S·22P₂S₅^[137], S/3,5-divinylbenzene copolymer^[138], S-C/super P carbon/Li₆PS₅Br^[139], S-carbon nanotubes/AB/Li₁₀GeP₂S₁₂^[45] and S-mesoporous carbon/thio-LISICON^[151]. According to these results, it can be concluded that composite cathodes benefit from improved diffusion, larger contact area, increased electronic and ionic conductivity and more suitable interfacial compatibility caused by ball milling, which is actually required to increase the contact area of electrode materials, decrease the interfacial resistance and enhance the performance of batteries.

Furthermore, other methods are employed to synthesize the composite cathode materials. For example, a series of sulfur-rich composite cathodes containing S and Li₃PS₄ prepared by solution reactions in tetrahydrofuran show good ionic conductivities and high electrochemical reversibility during cycling^[140], because the reaction between elemental sulfur and PS₄³⁻ anion can generate a new family of sulfur-rich compounds with high lithium-ion conductivity (10⁻⁵-10⁻⁶ S cm⁻¹). In order to improve the ionic conductivity of Li₂S cathodes, the core-shell nanostructure of Li₂S (core)-Li₃PS₄ (shell) was fabricated by a solution-based reaction^[141] and the reduced interfacial resistance and improved performance of batteries could be attributed to the innovative nanostructured materials. A favorable interface between the S-C composite cathode and LiBH₄ electrolyte could be realized by cold pressing, which allows for three-dimensional (3D) charge transfer in the cathode^[142]. Homogeneous nanocomposite electrodes consisting of Li₂S, carbon and polyvinylpyrrolidone prepared by a novel bottom-up method show outstanding mechanical and conducting properties^[143]. This is because the resulting nanoscale mixed-conductive network, consisting of ionic conductive SSEs and electronic conductive carbon, can effectively maintain the intimate contact between the cathode and electrolyte and improve the electronic conduction and Li-ion diffusion of the electrode. Introducing sulfur into the porous carbon replicas can form a 3D carbon matrix framework structure with high electronic conduction using a gas-phase mixing method^[129], which exhibits an improved battery energy density.

A novel Li₇La₃Zr₂O₁₂ nanoparticle/porous carbon foam synthesized by the one-step facile Pechini sol-gel method can serve as an ion/electron conductive matrix to construct a high-performance S-based cathode^[144]. The structural framework of graphene oxide/polyethylene glycol prepared by an esterification

Table 3. Components, preparation method and electrochemical performance of composite cathodes

| Composition of cathode materials | Solid electrolyte | Method | Performance (mA hg ⁻¹) | References |
|--|---|--|------------------------------------|------------|
| S/Cu ₂ S/acetylene-black(AB)/80Li ₂ S/20P ₂ S ₅ | 80Li ₂ S·20P ₂ S ₅ | Ball milling | 650 after 20 cycles | [120] |
| S/poly(ethylene oxide)(PEO)/AB | P(EO) ₂₀ Li(CF ₃ SO ₂) ₂ N-10 wt.% Y-LiAlO ₂ | Ball milling | 290 after 50 cycles | [121] |
| S/Carbon/PEO/acetonitrile | (PEO) ₆ LiBF ₄ /Al ₂ O ₃ | Ball milling | 400 after 10 cycles | [122] |
| S/AB/thio-LISICON (Li _{3.25} Ge _{0.25} P _{0.75} S ₄) | LISICON | Ball milling | 30 after 5 cycles | [123] |
| Li ₂ S/Cu/80Li ₂ S/20P ₂ S ₅ | 80Li ₂ S·20P ₂ S ₅ | Ball milling | 350 after 20 cycles | [124] |
| 80Li ₂ S/20P ₂ S ₅ /Cu | 80Li ₂ S·20P ₂ S ₅ | Ball milling | 60 after 50 cycles | [125] |
| S/AB/80Li ₂ S/20P ₂ S ₅ | 80Li ₂ S·20P ₂ S ₅ | Ball milling | 850 after 200 cycles | [126] |
| Li ₂ S/A /80Li ₂ S/20P ₂ S ₅ | 80Li ₂ S·20P ₂ S ₅ | Ball milling | 700 after 10 cycles | [127] |
| S/graphite | 80Li ₂ S·20P ₂ S ₅ | Ball milling | 400 after 20 cycles | [128] |
| S/carbon/Thio-LISICON | Thio-LISICON | Ball milling | 1000 after 50 cycles | [129] |
| Vapor-grown carbon fiber (VGCF)/S/ionic liquid/ α -Li ₃ PS ₄ | α -Li ₃ PS ₄ | Ball milling | 1230 after 50 cycles | [130] |
| S/activated carbon/P ₂ S ₅ | Li ₁₀ GeP ₂ S ₁₂ | Ball milling | 1042 after 10 cycles | [131] |
| S/super P carbon/Li ₆ PS ₅ Br | Li ₆ PS ₅ Br | Ball milling | 1080 after 50 cycles | [132] |
| sulfur/AB/75Li ₂ S·25P ₂ S ₅ | 75Li ₂ S·25P ₂ S ₅ | Ball milling | 450 after 20 cycles | [115] |
| S-C/Li ₆ PS ₅ Cl/super P | Li ₆ PS ₅ Cl | Ball milling | 400 after 20 cycles | [133] |
| S/C/Li ₇ P _{2.9} Mn _{0.1} S _{10.7} I _{0.3} | Li ₇ P _{2.9} Mn _{0.1} S _{10.7} I _{0.3} | Ball milling | 800 after 60 cycles | [116] |
| S-graphene oxide/Li _{9.54} Si _{1.74} P _{1.44} S _{11.7} Cl _{0.3} /carbon black | Li _{9.54} Si _{1.74} P _{1.44} S _{11.7} Cl _{0.3} | Ball milling | 827 after 60 cycles | [99] |
| Li ₂ S-VGCF/78Li ₂ S·22P ₂ S ₅ /Ketchen black conductive carbon | 78Li ₂ S·22P ₂ S ₅ | Ball milling | 600 after 20 cycles | [83] |
| Reduced graphene oxide-S/Li ₁₀ GeP ₂ S ₁₂ /AB | Li ₁₀ GeP ₂ S ₁₂ -75%Li ₂ S-24%P ₂ S ₅ -1%P ₂ O ₅ | Ball milling | 830 after 750 cycles | [84] |
| S/AB/70Li ₂ S·30P ₂ S ₅ | 70Li ₂ S·30P ₂ S ₅ | Ball milling | 673 after 5 cycles | [134] |
| Li ₂ S/super P carbon/VGCF/70Li ₂ S·30P ₂ S ₅ | 70Li ₂ S·30P ₂ S ₅ | Ball milling | 464 after 10 cycles | [135] |
| S-C-FeS ₂ /Li ₃ PS ₄ -LiI | Li ₃ PS ₄ -LiI | Ball milling | 800 after 20 cycles | [136] |
| S-carbon nanotubes/multi-wall carbon nanotubes/78Li ₂ S·22P ₂ S ₅ | 78Li ₂ S·22P ₂ S ₅ | Ball milling | 834.3 after 1000 cycles | [137] |
| S/3,5-divinylbenzene copolymer | Lithium-bis(fluorosulfonyl)imide/PEO | Ball milling | 800 after 50 cycles | [138] |
| S-C/super P carbon/Li ₆ PS ₅ Br | Li ₆ PS ₅ Br | Ball milling | 204 after 35 cycles | [139] |
| S-carbon nanotubes/AB/Li ₁₀ GeP ₂ S ₁₂ | Li ₁₀ GeP ₂ S ₁₂ /75%Li ₂ S-24%P ₂ S ₅ -1%P ₂ O ₅ | Ball milling | 660.3 after 400 cycles | [45] |
| Li ₃ PS ₄₊₅ | Li ₃ PS ₄ | Solution reaction | 700 after 400 cycles | [140] |
| Li ₂ S-Li ₃ PS ₄ | β -Li ₃ PS ₄ | Solution reaction | 402 after 100 cycles | [141] |
| S-Ketjen Black/ LiBH ₄ | LiBH ₄ | Cold-pressing | 630 after 50 cycles | [142] |
| Li ₂ S/C/Li ₆ PS ₅ Cl | Li ₆ PS ₅ Cl | Bottom-up approach | 830 after 60 cycles | [143] |
| S-carbon replica/ Li _{3.25} Ge _{0.25} P _{0.75} S ₄ | Li _{3.25} Ge _{0.25} P _{0.75} S ₄ | Gas-phase mixing and ball milling method | 500 after 10 cycles | [129] |
| S- Li ₇ La ₃ Zr ₂ O ₁₂ -C | Li ₇ La ₃ Zr ₂ O ₁₂ -PEO | Pechini sol-gel method | 700 after 200 cycles | [144] |
| Graphene oxide/polyethylene glycol @C/S | PEO-a metal-organic framework-LiTFSI | One-pot reaction | 531 after 100 cycles | [145] |
| S/acetylene black/Li _{3.25} Ge _{0.25} P _{0.75} S ₄ | Li _{3.25} Ge _{0.25} P _{0.75} S ₄ | High-temperature mechanical milling | 800 after 40 cycles | [146] |
| Carbon replica-S/Thio-LISICON | Thio-LISICON | Gas-phase mixing and ball | 500 after 10 cycles | [147] |

| | | | milling method | | |
|---|---|--|---|----------------------|-------|
| S-carbon replica/ $\text{Li}_{10.05}\text{Ge}_{1.05}\text{P}_{1.95}\text{S}_{12}$ | $\text{Li}_{10.05}\text{Ge}_{1.05}\text{P}_{1.95}\text{S}_{12}$ | | Combined mechanical and liquid-phase mixing | 1500 after 50 cycles | [148] |
| $\text{Li}_2\text{S-TiS}_2$ -electrolyte | Electrolyte | | Two-step dry/wet-mixing | 400 after 200 cycles | [103] |

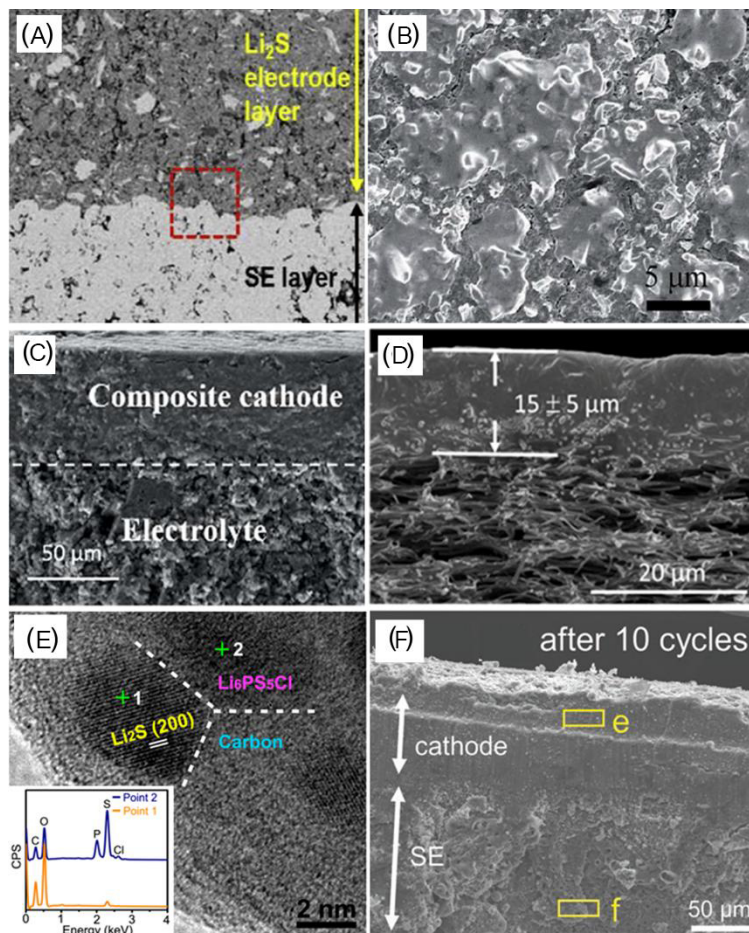


Figure 10. Cross-sectional SEM images exhibiting (A) the interface between a SSE and composites of Li_2S , AB and SE glass (reproduced with permission from [115]). (B) S-C- $\text{Li}_x\text{P}_{2.9}\text{Mn}_{0.1}\text{S}_{10.7}\text{I}_{0.3}$ composite (reproduced with permission from [116]). (C) Cathode layer after cycling (reproduced with permission from [117]). (D) Bilayer framework with a clear PEO/LLTO solid composite electrolyte layer (thickness of $15 \pm 5 \mu\text{m}$) (reproduced with permission from [118]). (E) High-resolution TEM image of $\text{Li}_2\text{S-Li}_6\text{PS}_5\text{Cl-C}$ sample and (F) cross-sectional SEM images of interlayer-modified Li_2S pellet (reproduced with permission from [119]).

reaction was used to fabricate graphene oxide/polyethylene glycol@C/S composite cathodes, which showed a long cycling life (capacity retention of 86.6%) after 100 cycles [145]. The introduction of graphene oxide and polyethylene glycol is beneficial for increasing the electronic conduction and Li-ion diffusion pathway in the cathode separately. A composite cathode of sulfur/AB/ $\text{Li}_{3.25}\text{Ge}_{0.25}\text{P}_{0.75}\text{S}_4$ was obtained by a high-temperature ball milling (443 K) method, which contributed to the generation of the reaction between S and the electrolyte and the formation of novel structural units [146].

Sulfur can be introduced into the mesopores of carbon replica by a combination method of gas-phase mixing and ball milling for preparing a carbon replica-S and $\text{Li}_{3.25}\text{Ge}_{0.25}\text{P}_{0.75}\text{S}_4$ composite electrode [147]. The employed carbon replica provides a good conductive framework for the composite cathode and the

resulting composite structure plays a critical role in improving the performance of the cathode. It has been reported that the combined mechanical and liquid-phase mixing can increase the ionic conduction pathway in cathode materials incorporating carbon replica, S and a solid electrolyte, resulting in improved electrochemical performance of the composite cathode^[148]. A simple two-step dry/wet-mixing method was reported by Chung et al. for preparing a cathode composite of homogeneous $\text{Li}_2\text{S}-\text{TiS}_2$ -electrolyte^[103], which enables the composites to realize an intimate contact between the conductive TiS_2 , active materials and the SSE. Consequently, all these strategies are expected to construct favorable interfaces to alleviate stain/stress and achieve ultrafast electronic and ionic pathways in solid-state battery systems.

Introducing a bifunctional ion-electron conducting layer between cathodes and SSEs

Intercalating a bifunctional ion-electron conducting layer between SSEs and cathodes offers another practical method to improve the interfacial compatibility of batteries^[152]. The conducting layer is composed of super P and PEO. An ASSLSB with a conducting layer thickness of 40 μm showed enhanced electrochemical properties (792.8 mAh g^{-1} after 50 cycles) and interfacial compatibility. A novel bilayer framework has been designed and fabricated by integrating a carbon nanofiber/sulfur composite with a ceramic $\text{Li}_{0.33}\text{La}_{0.557}\text{TiO}_3$ nanofiber-PEO solid electrolyte, which showed an intimate and sufficient phase contact of active materials and electrolyte and can function as both the cathode and electrolyte for high-performance ASSLSBs^[118]. Furthermore, it has been demonstrated that modifying the interface between the cathodes and SSEs with a highly concentrated solvate electrolyte as a Li^+ -conducting interfacial layer, acetonitrile-lithium-bis(trifluoromethane sulfonyl)imide:1,1,2,2-tetrafluoroethyl 2,2,3,3-tetrafluoropropyl ether, can promote the sufficient interfacial contact of electrodes and electrolytes^[119]. A multi-channel continuous electronic/ionic conductive network composed of the composite of a reduced graphene oxide-vanadium tetrasulfide nanostructure coated with $\text{Li}_7\text{P}_3\text{S}_{11}$ solid electrolyte nanoparticles can also contribute to the improvement of the electronic/ionic conductivity and interfacial contact^[153].

Based on the above research, it can be concluded that ASSLSBs based on composite cathodes exhibit higher electrochemical performance than cells constructed with pure active materials. A suitable phosphorus/sulfur (P/S) ratio of ISSEs in the composite cathodes is very important for a high ionic conductivity, which can increase the reactivity of the sulfur, resulting in an improved battery performance^[154]. The interfacial compatibility between SSEs and cathodes greatly depends on their composition and the structure of composite cathode materials. The composite cathode materials composed of active materials and Li-ion and electronic conductors can combine the advantages of each species to improve cathode/electrolyte interfacial properties. The design and fabrication of smart cathode/electrolyte integrated architectures to decrease the interfacial resistance will be the direction of future research. Further understanding of their interfacial construction is important for accelerating the development of ASSLSBs.

Lithium anode side

In addition to the strategies conducted for the improvement of interfacial compatibility between SSEs and cathodes, the issues related to the interface between Li anodes and SSEs should also be considered in ASSLSBs. A solid electrolyte interphase layer is easily generated at the anode/SSE interface due to the decomposition products of the SSE, which have lower ionic conductivity and result in increased interfacial resistance. A “dot-dot” interfacial contact can cause non-uniform Li dissolution/deposition, reduce the utilization of Li metal and result in a high interfacial resistance between a Li anode and SSEs, which is a serious problem for ASSLSBs. Furthermore, the interfacial resistance is obviously related to the interface voids and grain boundaries. In order to decrease the anode/SSE interfacial resistance and promote their interfacial contact, numerous methods have been developed, such as introducing protective interlayers and fabricating composite SSEs [Figure 4].

Introducing interface layers between lithium anodes and SSEs Metal-based thin films

Since the Li metal anode has the most negative electrochemical potential, it can easily react with most SSEs to form a metastable interface, resulting in poor Li-ion diffusion. In order to alleviate the interfacial reactions between the SSE and lithium electrode^[155], metal thin films were introduced on the SSE surface, including Li^[156], Au^[157], Al^[158], In^[126], Ge^[136], Sn^[159] and Mg^[160]. These are effective in constructing homogeneous interfaces between the anode and SSEs, because the metal can react with Li to form a Li-metal alloy layer, effectively decreasing the generation of grain boundaries and voids at the SSE/anode interface and improving their interfacial compatibility. For example, Au thin films were employed as an ideal interface between the SSE and anode, because Au shows good interfacial wetting with them^[161]. In addition, an ultrathin, artificial intermediary Al layer was used to modify the interface of the garnet solid electrolyte and Li metal, and the formed Li-Al alloy interface layers play a key role in improving the Li wettability of SSE and reducing their interfacial resistance^[158]. Similarly, a favorable interface between the SSE and anode can be constructed by alloying Li metal with Ge, and the formed Li-Ge alloy interface layer has a high Li-ion conductivity^[136]. Since Sn has a high lithium diffusion rate and ductility, it can be inserted into the electrode/anode interface to construct a suitable interfacial phase and decrease the interfacial resistance^[159]. A Li-rich Li-Mg alloy was deposited on the surface of a SSE and employed as an anode for ASSLSBs, because the Li-Mg framework can construct continuous Li-ion/electron dual-conductive pathways at the anode/SSE interface^[160] [Figure 11A-J]. Therefore, it is expected that more metals that are miscible with Li can be used as suitable interphases to construct ideal anode/electrode interfaces.

Inorganic materials

Many inorganic materials, including Al₂O₃^[158,159], ZnO^[113], amorphous Si^[166], graphite^[32,167,168], LiH₂PO₄^[169], BN^[161] and Li₃N^[170], have outstanding reactivity with molten lithium, which can serve as a surface modification layer of garnet SSE to fill the gap between the SSE and lithium electrode. The resulting intimate contact between lithium and garnet SSE leads to a low interfacial resistance decrease. Inserting an ultrathin Al₂O₃ layer into the anode/electrolyte interface can promote the molten Li metal to be uniformly deposited on the surface of SSE and prevent the generation of interfacial void space, resulting in an improvement in the interfacial wetting and stability^[156,157] [Figure 11K and L]. Furthermore, the surface wettability of a SSE can be significantly improved by a ZnO coating layer, because it can react with the molten Li metal to form a Li-Zn alloy layer to enhance the interfacial contact between the SSE and lithium electrode^[113]. In addition, an electron/ion dual-conductive framework formed by a reaction between graphite and the molten Li metal can ensure good interfacial contact with the SSE^[32,167,168]. Since a LiH₂PO₄ protective layer in situ constructed by a manipulated reaction between Li anode and Li₁₀GeP₂S₁₂ can effectively prevent uncontrollable interfacial layer growth, enhance the contact area of electrode/electrolyte and benefit the diffusion of mixed ionic-electronic reactants into the inner of electrolyte, it is considered as an ingenious interfacial reengineering strategy for reducing the anode/SSE interfacial resistance^[169]. A BN nanofilm, which has good insulation and ionic conductivity, was also employed as a protecting layer to reduce the reduction of the SSE by Li metal and stabilize the electrolyte/anode interface^[161]. Coating Li₃N onto the Li metal surface could be an effective method for constructing better SSE-lithium wetted interfaces^[170] because Li₃N has high Li-ion conductivity and is easily prepared by a direct reaction between Li metal and nitrogen at room temperature. Consequently, the surface reactions between the introduced protective interlayers and the Li metal play an essential role in improving the electrode/anode interfacial compatibility and Li-ion and electronic conductivity^[171].

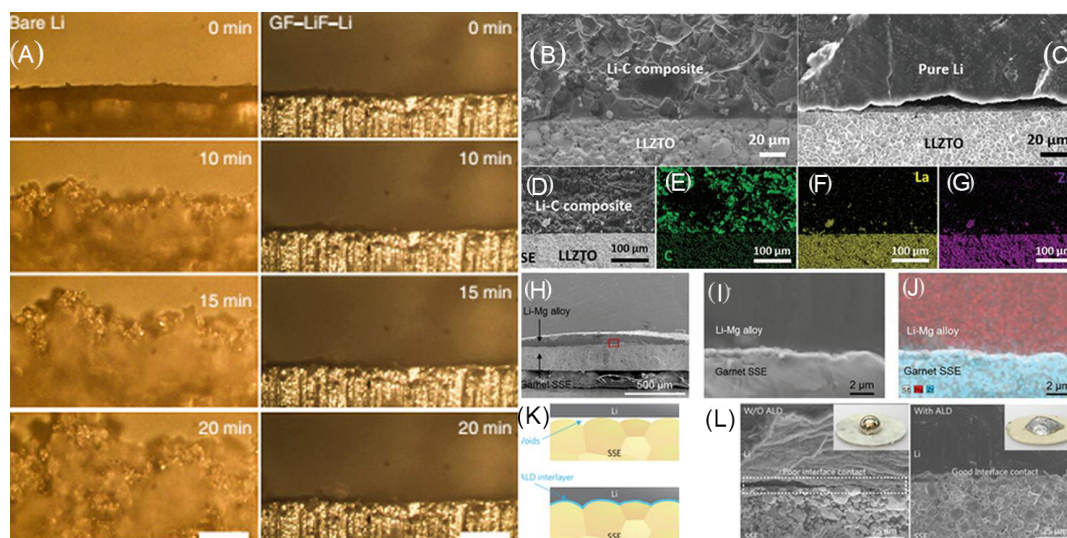


Figure 11. (A) *In-situ* optical microscopy visualization of bare Li (left column) and graphite fluoride-LiF-Li (right column) electrolyte interface in different time periods during cycling on symmetric cells (reproduced with permission from^[162]). Comparison between bare Li and Li/graphite interfacial behaviors with SSE pellet. SEM images of (B) Li-C/SSE and (C) bare Li/SSE interfaces and (D-G) elemental mappings of the Li-C/SSE interface (reproduced with permission from^[163]). (H) Cross-sectional SEM image and (I) high-magnification cross-sectional SEM image of Li-Mg alloy melted on the SSE and (J) corresponding elemental mapping by EDX at the interface (reproduced with permission from^[164]). (K) Schematic of molten Li wetting behavior for pure SSE and ALD- Al_2O_3 -coated SSE, respectively, and (L) SEM images of the SSE/Li metal interface [without ALD- Al_2O_3 coating (left) and with ALD- Al_2O_3 coating (right)] (reproduced with permission from^[165]).

Organic polymer electrolytes

Although various protective interlayers have been successfully introduced into the SSE/anode interface to effectively decrease the interfacial resistance, the generation of unnecessary side reactions and elemental infiltration during cycling has a potentially negative impact on the performance of ASSLSBs^[172]. Therefore, the introduction of PEO-based electrolytes with high ionic conductivity, excellent mechanical stability and good thermal stability between the Li metal and inorganic SSE promises a significantly increased contact area for the electrolyte/electrodes^[173-176]. For example, an adaptive buffer layer (ABL) consisting of low molecular weight polypropylene carbonate, PEO and lithium salt was proposed to make an intimate interfacial contact between the solid polymer electrolytes and Li metal anode during battery cycling^[175] because the ABL has high viscosity and ionic conductivity. Yu *et al.* demonstrated that introducing a 3D gel polymer electrolyte at the interface between $\text{Li}_{1.5}\text{Al}_{0.5}\text{Ge}_{1.5}(\text{PO}_4)_3$ pellets and lithium metal anodes can reduce interfacial resistance and suppress the volumetric change of the anodes during cycling^[175]. It has been reported that a PEO-based solid polymer electrolyte-coated diatomite-derived lithium silicide-Li composite can act as a hierarchically structured, stable and dendrite-free Li metal-based hybrid anode for high-performance ASSLSBs^[176]. Overall, the PEO-based layer can resist the side reactions between solid electrolytes and lithium to some extent^[177]; however, it is noteworthy that Li metal may destroy the PEO-based protective layer because of its reducibility. Thus, it could be expected that more effective strategies will be developed for constructing suitable interfaces between Li anodes and SSEs^[178].

Others

A novel wetting agent, namely, a 1.5 M LiTFSI/Pyr₁₃TFSI ionic liquid, was successfully employed to enhance the interfacial stability between the $\text{Li}_{10}\text{SnP}_2\text{S}_{12}$ solid electrolyte and Li metal interface and the cycling performance of symmetric cells^[36]. Recently, a 3D electronic and ionic mixed conducting interlayer composed of a Sn/Ni alloy layer-coated Cu nanowire network showed the capability to improve the

interfacial affinity in ASSLSBs^[179]. Furthermore, a graphite fluoride-lithium fluoride-Li composite as a dendrite-free lithium anode for Li-ion batteries exhibits long-term stability in ambient air^[155].

The introduction of various interface layers with high ionic conductivity between Li anodes and SSEs has been demonstrated to be an effective method for wetting the interface and achieving intimate contact, which may be the main strategy to reduce interfacial resistance^[180].

Fabricating composite SSEs between sulfur cathodes and lithium anodes

An increasing number of investigations have focused on composite electrolytes, which are promising for overcoming issues related to dendrite growth, the shuttle effect of sulfur and the large interfacial resistance in practical ASSLSBs because they have the combined advantages of inorganic and organic electrolytes, such as good interfacial contact, high ionic conductivity and excellent thermal stability. The inorganic portion can afford continuous Li-ion transfer channels in an organic-based composite and the organic portion with flexibility improves the interfacial contact to reduce the interfacial resistance^[181].

Composite solid electrolytes composed of a PEO-based polymer and an inorganic Li-ion conductor possess good ionic conductivity and interfacial stability and have been employed as electrolytes for ASSLSB cells showing good cycle stability. Example composites include P(EO)₂₀Li(CF₃SO₂)₂N-10 wt.%Y-LiAlO₂^[182], PEO-lithium bis(trifluoromethanesulfonyl)imide (PEO₁₈LiTFSI)/nanosilica/N-methyl-N-propylpiperidinium-bis(trifluoromethanesulfonyl)imide (PP13TFSI)^[183], polyacrylonitrile-LiClO₄/15 wt.% Li_{0.33}La_{0.557}TiO₃ nanowire^[184], 3D garnet-type Li_{6.4}La₃Zr₂Al_{0.2}O₁₂/PEO^[185], Li_{1.5}Al_{0.5}Ge_{1.5}(PO₄)₃/PEO-based gel-polymer^[186], Li_{10+x}SnP₂S₁₂/P(EO)₃/Li^[187], poly(vinylidene fluoride-hexafluoropropylene) (PVDF-HFP)/Li_{1.5}Al_{0.5}Ti_{1.5}(PO₄)₃ (LATP) nanoparticles^[188], well-aligned Li_{0.33}La_{0.557}TiO₃ nanowires/polymer electrolyte^[188], inorganic Al₂O₃ fillers/lithium bis(fluorosulfonyl)imide-PEO/Li-ion conducting glass-ceramic^[144], Li₇La₃Zr₂O₁₂/carbon foam/PEO^[189], Li_{0.33}La_{0.557}TiO₃ nanofibers/sulfonamide lithium-PEO^[189], Li₇P₃S₁₁/PEO-LiClO₄^[190], Li_{6.4}La₃Zr_{1.4}Ta_{0.6}O₁₂/PEO/LiTFSI^[191] and PEO/LiTFSI/Li_{1.4}Al_{0.4}Ge_{1.6}(PO₄)₃^[192].

This improved performance may be attributed to the synergistic effect of the inorganic and organic portions of the composites. For example, the improvement of PEO₁₈LiTFSI conductivity caused by the addition of nano-SiO₂ is due to the surface interaction between ionic species and O/OH groups at the filler surface and the addition of PP13TFSI results in the generation of a passivation film with lower resistance^[183]. Li_{0.33}La_{0.557}TiO₃ nanowire fillers with high ionic conductivity and large aspect ratio filled in a polyacrylonitrile-LiClO₄ electrolyte can form fast conductive networks and Li-ion diffusion pathways^[184]. However, the agglomeration of one-dimensional ceramic fillers could be an issue in fabricating homogeneous composite solid electrolytes for their practical application. In order to avoid the agglomeration of fillers, 3D ceramic networks were soaked into Li salt-polymer solutions for fabricating the composite solid electrolytes, which can afford continuous channels for Li⁺ transfer in the electrolytes and structural reinforcement^[185]. Since LATP nanoparticles have a strong impact on the recrystallization kinetics of the polymer-based matrix to promote local amorphous areas and enhance the stability of the long-term structure and PVDF-HFP has large dielectric constant, good interfacial compatibility and high ionic conductivity, they have been chosen to fabricate a novel composite gel polymer electrolyte^[186]. Introducing the well-aligned inorganic Li⁺-conductive nanowires into the solid polymer electrolytes can result in an increase in ionic conductivity, because of a fast ion conduction pathway without crossing junctions on the surface of the well-aligned nanowires^[189]. A composite electrolyte additive, the Li₇La₃Zr₂O₁₂ nanoparticle-decorated carbon foam, can be used as both the interfacial stabilizer and filler to improve ionic and electronic conductivity of the electrolyte/electrode interface^[144]. PEO-LiClO₄, with good electrochemical stability, can effectively prevent the reaction between the Li₇P₃S₁₁ glass-ceramic electrolyte and lithium,

which is added to the SSE to reduce the interfacial resistance between the Li metal anode and SSE^[193]. Adding $\text{Li}_{6.4}\text{La}_3\text{Zr}_{1.4}\text{Ta}_{0.6}\text{O}_{12}$ to a polymer matrix can contribute to an improvement in interfacial compatibility and Li-ion conductivity because of the bonding of the PEO polymer matrix to the anode and rigid $\text{Li}_{6.4}\text{La}_3\text{Zr}_{1.4}\text{Ta}_{0.6}\text{O}_{12}$ particles with PEO chain segments^[191].

Composite electrolytes are enlightening in improving the electrochemical performance of ASSLSB cells because of the combined advantages of both ceramics and PEO polymers. In the composites, a host PEO polymer matrix filled with inorganic Li-ion conductors presents new recrystallization kinetics of the polymer chains and increases more flexible local chains in the amorphous phase, resulting in enhanced electrochemical stability and interfacial compatibility. However, the relatively high operating temperature of composite solid electrolytes restricts their practical application, which needs to be further reduced^[194].

ADVANCED ANALYTICAL CHARACTERIZATION

In-situ and *ex-situ* characterization methods have been widely used for characterizing all-solid-state Li batteries^[195-201], including X-ray absorption spectroscopy, XRD, Raman spectroscopy, nuclear magnetic resonance spectroscopy, neutron diffraction, transmission X-ray microscopy, SEM, TEM and atomic force microscopy (AFM). These characterization techniques are powerful tools to investigate and understand interfacial issues in solid-state batteries and can afford deep insights into their electrochemical behavior, electronic state, structure and morphology at the atomic level^[202].

Ex-situ techniques

Ex-situ characterization is a relatively low-cost and convenient method to reveal the evolutions at the interfaces of electrodes. SEM and TEM have been used for characterizing the interfacial properties of electrodes/SSEs, including the structural changes and chemical instability, and are useful tools suitable for comprehensively understanding the role of interfaces in solid-state lithium batteries at the atomic level.

SEM/EDS analysis of the solvate interlayer-modified Li_2S pellet has revealed that the use of a solvate can enhance the wettability of the cathode and the solvate diffuses into the void spaces of the cathode and grain boundaries of the SSE during cell cycling, resulting in a decrease in the interfacial impedance of the cell [Figure 12A and B]^[199]. TEM imaging and electron energy-loss spectroscopy mapping demonstrated that the SSE surface with the Al_2O_3 coating has good wettability with Li metal. Al can permeate into the SSE surface and form a lithiated-alumina transition layer [Figure 12C and D]^[20,158]. Furthermore, electrochemical impedance spectroscopy (EIS) is a powerful tool to investigate the interfacial behavior between the electrode and SSE and afford useful information on Li-ion diffusion in all-solid-state Li batteries^[195]. It has been reported that the interfacial behavior, including stability and resistance between electrodes and SSEs during cycling, can be assessed by the changes of semicircles in the low- and high-frequency ranges [Figure 12E and F]^[197,203]. Neutron depth profiling is used to diagnose short circuits in symmetric solid-state batteries and analyze the Li-ion transport behavior of solid-state batteries^[198].

In-situ techniques

Although most characterization methods for investigating all-solid-state Li batteries are *ex-situ* experiments, in order to further understand the electrochemical phenomenon and structural evolution of the interfaces of the solid-state systems during the cycling process, more advanced in situ/operando characterization techniques are required. These techniques will benefit researchers attempting to reveal the interfacial reaction kinetics and decay mechanism of solid-state batteries in real time. In comparison with *ex-situ* characterization, in situ/operando characterization techniques including S/TEM can dynamically detect the interfacial structural evolution and phase transitions in a nonequilibrium state during charging and

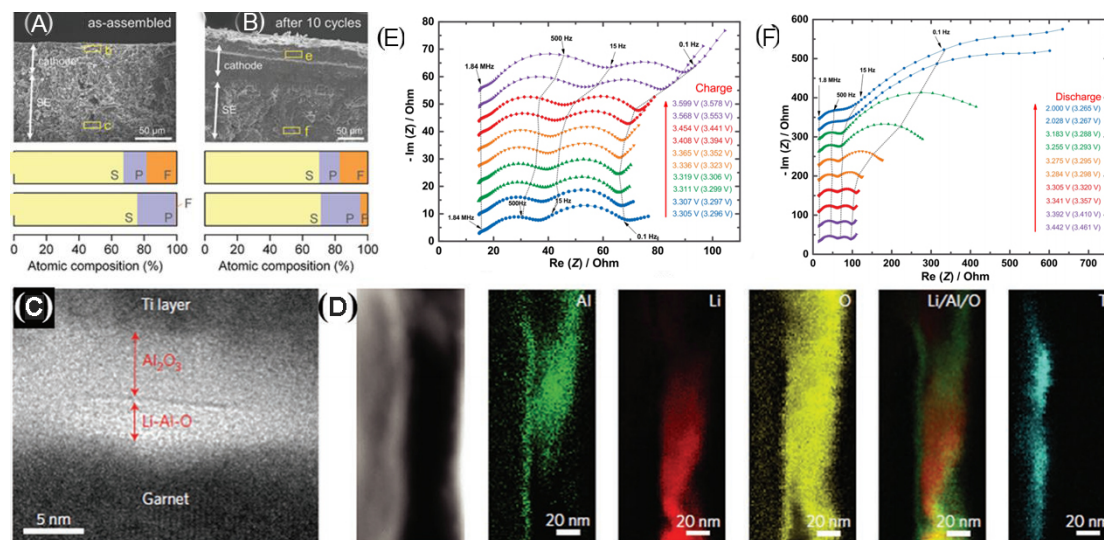


Figure 12. SEM images of (A) pristine solvate interlayer-modified Li₂S pellet and (B) interlayer-modified Li₂S pellet after ten cycles. EDS analysis shown in (A) and (B) (yellow rectangle regions). Comparing relative F content (F atoms from LiTFSI and TTE) at different regions can confirm the possible infiltration of the solvate across the pellet (reproduced with permission from^[193]). (C) TEM cross-sectional image for the interface of an ALD-Al₂O₃-coated SE with Ti protection layer. (D) EELS maps (Al, Li, O, overlap of Al and Li, and Ti, respectively) at the interfacial cross section (reproduced with permission from^[201]). Characterization of an SSB with LNTO-coated LiCoO₂ during the charge (E) and discharge (F) process by EIS, which was carried out after a 1 h charge and a 30 min rest (stacked Nyquist plots) and the galvanostatic charge was carried out at 0.1 C (reproduced with permission from^[196]).

discharging, directly provide real-time lithiation/delithiation information and help demonstrate the structure-performance relationships of ASSLSBs and electrochemical reaction mechanism in real time.

Recently, the interfacial issues in solid-state systems have been studied using *in situ/operando* characterization techniques. It has been demonstrated that the electrochemical reaction mechanism in ASSLSB with a sulfide-based SSE by *in-situ* SEM characterization^[200]. This reveals that homogeneous lithium deposition on the SE and the suppression of the dendritic growth are critical to obtaining the highly reversible lithium deposition and dissolution reaction. A valuable amount of information regarding the electrochemical behaviors on the interfaces between lithium phosphorus oxynitride and metallic lithium can be provided by *in-situ* XPS. Gong *et al.* constructed a working LiCoO₂/LLZO/Au ASS battery by using a combination of a state-of-the-art chip-based *in-situ* TEM holder and focused ion beam milling to observe the structural evolution of electrodes during cycling on an atomic scale with TEM [Figure 13]^[201]. These *in-situ* STEM results demonstrated that good interfacial contact between the electrode and electrolyte is very important to achieving high-performance ASSLSBs.

Advanced *in-situ* and *ex-situ* characterization methods can benefit researchers in understanding solid interfacial reactions, the interfacial structural evolution, the interfacial phase transitions and fundamental ion-transport mechanisms at interfaces, and overcome interfacial issues, including the interfacial compatibility, interface stability and interfacial resistance in the solid-state systems, revealing the reaction kinetics and decay mechanism of ASSLSBs, and affording guidance to design and optimize high-performance ASSLSBs. Furthermore, a combination of different *in-situ* and *ex-situ* characterization methods is desperately required to further reveal the evolutions at the interfaces.

COMMERCIALIZING PROGRESS IN ASSLSBS

The high theoretical energy density (~2500 Wh kg⁻¹), low cost, natural abundance, environmental benignity

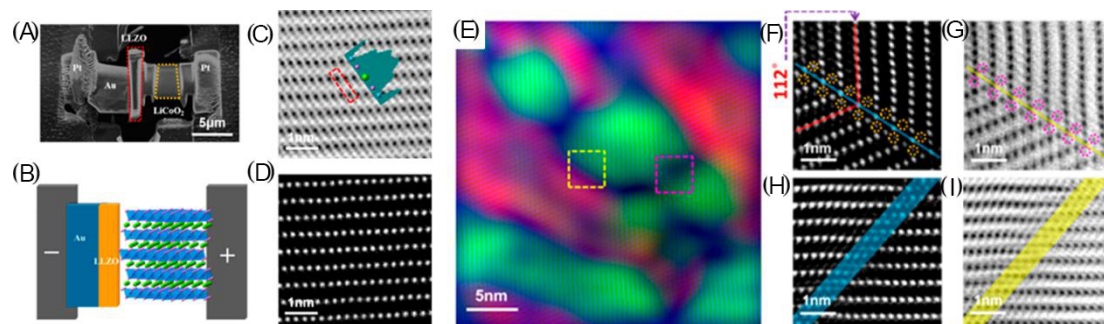


Figure 13. (A) *In-situ* observation of a micro-electro-mechanical system device nanochip using the focused ion beam to apply the electric field (from left to right are the anode, SSE and cathode) and the (B) corresponding schematic. (C) Annular bright-field (ABF) and (D) high-angle annular dark-field (HAADF) images of a pristine cathode annular. The corresponding line profile acquired at the red dashed line rectangular zone is shown in panel (C) with both lithium and oxygen contrast. Lithium, oxygen and cobalt ions are represented as green, purple and cyan balls, respectively, in panels (B) and (C). (E) HAADF image of the delithiated cathode colored in blue using the GPA method and two orientations colored with green and red. Panels (F) and (G) are zoomed-in micrographs of the yellow, dashed-line, rectangular area. Panels (H) and (I) are zoomed-in micrographs of the pink, dashed-line, rectangular area. For both boundaries, a contrast in the lithium layer in both the HAADF and the ABF micrograph is shown, suggesting heavy atoms are present in the lithium layer. The basal planes of the two crystals that meet at an angle of 112° are shown in panels (F) and (G) (reproduced with permission from^[201]).

of sulfur and high safety make ASSLSBs more commercially viable than other battery systems and are expected to play a key role in the future development of energy storage systems. However, their performance promotion achieved at the laboratory level could offer a false sense of research direction, because there is a significant gap between practical pouch cells and laboratory coin cells under realistic conditions. Data collected from coin cell testing under ideal conditions is clearly far from the requirement of practical applications. To guide the rational design of ASSLSB engineering, the effect of the required performance parameters close-to-application multilayer-pouch cells on the gravimetric and volumetric energy densities and safety should be evaluated and analyzed.

To realize practical energy densities, the thickness of both the electrode and electrolyte layers is required to be thinner than $50 \mu\text{m}$ and sulfur loading higher than $4\text{-}5 \text{ mg cm}^{-2}$. Furthermore, scalable continuous roll-to-roll methods are necessary for practical pouch cell manufacturing [Figure 14]^[204]; however, few reports on such methods to build ASSLSBs with sulfide-based solid electrolytes have been presented^[205].

Several interesting methods have so far been proposed to efficiently promote the commercialization of ASSLSBs, including thin-film, wet (solvent-based) and melt-casting methods. Despite their several advantages to fabricating solid-state micro-batteries, such as the desired thicknesses, high densification and good interface compatibility, the cost control for the extensive application of thin-film methods is very significant^[78,98,206]. In terms of the interfacial compatibility between the electrodes and electrolytes, wet (solvent-based) methods show obvious advantages. Solid electrolytes and various components of composite electrodes can be well mixed directly from liquid suspensions or solutions to form self-assembled films after subsequent evaporating. It is noteworthy that the mixing protocols should be carefully considered to realize a homogeneous distribution of SSEs and electrode materials^[207]. In addition, it is believed that the direct solidification of the solid electrolyte into the desired shape and thickness, namely, melt casting, could be a feasible method to improve the interface compatibility; however, its application remains uncertain because such SSEs are required to form stable melts at low temperatures.

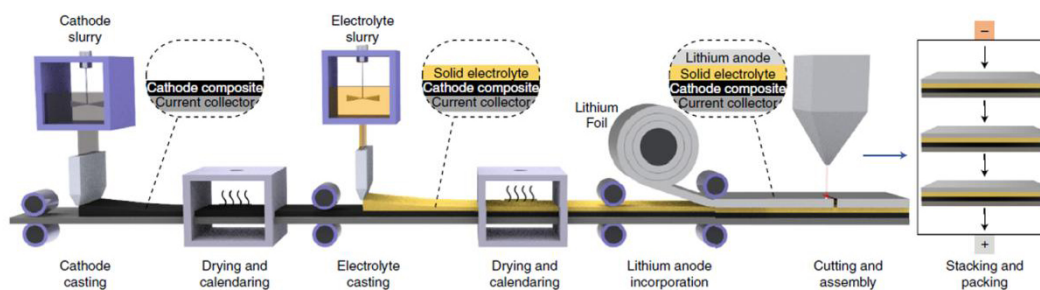


Figure 14. Schematic illustration of mass manufacturing process of ASSLSBs (reproduced with permission from [204]).

Finally, in comparison with Li-ion batteries, a number of disadvantages of ASSLSBs cannot be ignored in their practical application, such as lower volumetric energy density (682.3 vs. 727.5 Wh L⁻¹), considerable lithium excess, the insulating nature of sulfur, the large dosage of electrolyte, safety hazards, poor cycle life, poor low-temperature performance and serious self-discharge, which are more critical challenges for ASSLSB development.

Overall, the commercial viability of ASSLSBs should be improved with advanced electrodes and electrolyte materials, rational structural designs and smart manufacturing methods. Developing a “perfect” battery system could contribute to cutting costs and time in the electrical market. However, a substantial investment would also be required to accelerate the commercialization of ASSLSBs. Since parts of the advantages of ASSLSBs system are lost when evaluated more practically, it could possibly take a couple of years for ASSLSBs to be as broadly available as commercial Li-ion batteries are today.

CONCLUSIONS AND PERSPECTIVE

This review summarizes and discusses the origin and issues of electrode/SSE interfaces are summarized and discussed, introduces strategies for resolving interfacial issues and gives an overview of advanced analytical characterization methods. Despite ASSLSBs exhibiting excellent potential applications in electric energy storage devices after decades of development, they still face great challenges, including large interfacial impedance, poor interfacial compatibility, Li dendrite formation and a poor understanding of the interfacial properties, which greatly hinder the performance improvement of ASSLSBs. Therefore, efforts aimed at improving the interfacial stability, decreasing the impedance of the interfaces and understanding interfacial electrochemical behavior are critically important to enable ASSLSBs for their practical applications.

Generally, the inherent disadvantages of interfaces, including grain boundaries, voids and space charge layers between the electrodes and electrolyte, easily cause uneven current distribution at the interface, leading to large interfacial resistance, seriously affecting the electrochemical performance of ASSLSBs. Advanced strategies have been developed to modify and optimize the interfaces in ASSLSBs for overcoming the challenges deriving from the interfaces between electrodes and electrolytes; however, designing and constructing an ideal interface of the electrode/electrolyte with stable structure, high ionic conductivity and small resistance are still critically important. Therefore, in order to achieve the goal of high-performance ASSLSBs, the future research interest in the field of electrode/electrolyte interfaces is suggested as follows:

(1) Since the type and microstructure of interlayer materials are the keys to the interfacial properties, the next stage is to select and synthesize the advanced interlayer materials with good electrochemical stability, excellent mechanical behavior and fast conductive networks and Li⁺ diffusion pathways.

(2) Inorganic/inorganic composite electrolytes are also expected to resolve the issues associated with the electrode/electrolyte interface, such as Li dendrite penetration, poor interfacial compatibility and large interfacial resistance.

(3) Building smart electrode/electrolyte integrated architectures to suppress the shuttle effect of Li polysulfides, alleviate lithium dendrites growth and improve ionic conductivity and interfacial capability could be a direction of future research.

(4) The fundamental understanding of interfacial reaction, components and structure of interfacial products and their various influence on interfacial electrochemical behavior and mechanisms is very important for the future development of ASSLSBs.

(5) The interfacial evolution, role and dynamic characteristics should be investigated and understood by the advanced characterization techniques during charge-discharge cycling, such as *in-situ* TEM, XPS, SEM, AFM, XRD and operando UV-vis spectroscopy.

(6) The combination of experimental and theoretical calculation methods should be used to understand the interfacial properties of ASSLSBs.

In addition, future research should focus on the loading of the sulfur cathode, which needs to be increased for the high energy and power density of ASSLSBs. Much more work can be required to develop advanced fabrication approaches, design realistic test cells, optimize the component ratios and balance the relationship between safety and performance. Novel science and technology will help to drive the commercial development of ASSLSBs.

DECLARATIONS

Author's contributions

Methodology, conceptualization and writing - original draft: Tao T

Data curation: Tao T, Zheng Z, Gao Y

Writing - review & editing: Zheng Z, Gao Y

Formal analysis: Tao T, Zheng Z, Gao Y, Yu B, Fan Y, Chen Y, Huang S, Lu S

Availability of data and materials

Not applicable.

Financial support and sponsorship

This work was supported by Guangdong Natural Science Foundation, China (Grant No. 2022A1515010015, 2019A1515012041), the Natural Science Foundation of China (Grant No. 51372042, 51872053, 51920105004), the NSFC-Guangdong Joint Fund (Grant No. U1501246), Guangdong Provincial Natural Science Foundation (Grant No. 2015A030308004) and the Discovery program from the Australian Research Council.

Conflicts of interest

All authors declared that there are no conflicts of interest.

Ethical approval and consent to participate

Not applicable.

Consent for publication

Not applicable.

Copyright

© The Author(s) 2022.

REFERENCES

1. Takada K. Progress and prospective of solid-state lithium batteries. *Acta Materialia* 2013;61:759-70. DOI
2. Song MK, Cairns EJ, Zhang Y. Lithium/sulfur batteries with high specific energy: old challenges and new opportunities. *Nanoscale* 2013;5:2186-204. DOI PubMed
3. Lin Z, Liang C. Lithium-sulfur batteries: from liquid to solid cells. *J Mater Chem A* 2015;3:936-58. DOI
4. Pang Q, Liang X, Kwok CY, Nazar LF. Advances in lithium-sulfur batteries based on multifunctional cathodes and electrolytes. *Nat Energy* 2016;1. DOI
5. Wang Y, Sahadeo E, Rubloff G, Lin C, Lee SB. High-capacity lithium sulfur battery and beyond: a review of metal anode protection layers and perspective of solid-state electrolytes. *J Mater Sci* 2019;54:3671-93. DOI
6. Yan M, Wang W, Yin Y, Wan L, Guo Y. Interfacial design for lithium-sulfur batteries: from liquid to solid. *Energy Chem* 2019;1:100002. DOI
7. Kasemchainan J, Zekoll S, Spencer Jolly D, et al. Critical stripping current leads to dendrite formation on plating in lithium anode solid electrolyte cells. *Nat Mater* 2019;18:1105-11. DOI PubMed
8. Zhang W, Zhang Y, Peng L, et al. Elevating reactivity and cyclability of all-solid-state lithium-sulfur batteries by the combination of tellurium-doping and surface coating. *Nano Energy* 2020;76:105083. DOI
9. Nie K, Hong Y, Qiu J, et al. Interfaces between cathode and electrolyte in solid state lithium batteries: challenges and perspectives. *Front Chem* 2018;6:616. DOI PubMed PMC
10. Lou S, Zhang F, Fu C, et al. Interface issues and challenges in all-solid-state batteries: lithium, sodium, and Beyond. *Adv Mater* 2021;33:e2000721. DOI PubMed
11. Sun Y, Huang J, Zhao C, Zhang Q. A review of solid electrolytes for safe lithium-sulfur batteries. *Sci China Chem* 2017;60:1508-26. DOI
12. Judez X, Zhang H, Li CM et al. Review-solid electrolytes for safe and high energy density lithium-sulfur batteries: promises and challenges. *J Electrochem Soc* 2018;165:A6008-16. DOI
13. Tian Y, Shi T, Richards WD, et al. Compatibility issues between electrodes and electrolytes in solid-state batteries. *Energy Environ Sci* 2017;10:1150-66. DOI
14. Gauthier M, Carney TJ, Grimaud A, et al. Electrode-electrolyte interface in Li-ion batteries: current understanding and new insights. *J Phys Chem Lett* 2015;6:4653-72. DOI PubMed
15. Luntz AC, Voss J, Reuter K. Interfacial challenges in solid-state Li ion batteries. *J Phys Chem Lett* 2015;6:4599-604. DOI PubMed
16. Sang L, Bassett KL, Castro FC, et al. Understanding the effect of interlayers at the thiophosphate solid electrolyte/lithium interface for all-solid-state Li batteries. *Chem Mater* 2018;30:8747-56. DOI
17. Xiao Y, Wang Y, Bo S, Kim JC, Miara LJ, Ceder G. Understanding interface stability in solid-state batteries. *Nat Rev Mater* 2020;5:105-26. DOI
18. Zhang X, Cheng X, Zhang Q. Advances in interfaces between Li metal anode and electrolyte. *Adv Mater Interfaces* 2018;5:1701097. DOI
19. Umeshbabu E, Zheng B, Yang Y. Recent progress in all-solid-state lithium-sulfur batteries using high Li-Ion conductive solid electrolytes. *Electrochem Energ Rev* 2019;2:199-230. DOI
20. Zhang C, Feng Y, Han Z, Gao S, Wang M, Wang P. Electrochemical and structural analysis in all-solid-state lithium batteries by analytical electron microscopy: progress and perspectives. *Adv Mater* 2020;32:e1903747. DOI PubMed
21. Yue J, Yan M, Yin Y, Guo Y. Progress of the interface design in all-solid-state Li-S batteries. *Adv Funct Mater* 2018;28:1707533. DOI
22. Wu Z, Xie Z, Yoshida A, et al. Utmost limits of various solid electrolytes in all-solid-state lithium batteries: a critical review. *Renew Sustain Energy Rev* 2019;109:367-85. DOI
23. Xu L, Tang S, Cheng Y, et al. Interfaces in solid-state lithium batteries. *Joule* 2018;2:1991-2015. DOI
24. Hu Y-, Raistrick ID, Huggins RA. Ionic conductivity of Lithium orthosilicate -Lithium phosphate solid solutions. *J Electrochem Soc* 1977;124:1240-2. DOI
25. Shannon R, Taylor B, English A, Berzins T. New Li solid electrolytes. *Electrochim Acta* 1977;22:783-96. DOI
26. Hong H. Crystal structure and ionic conductivity of $\text{Li}_{14}\text{Zn}(\text{GeO}_4)_4$ and other new Li^+ superionic conductors. *Mater Res Bulletin* 1978;13:117-24. DOI

27. Kato Y, Hori S, Saito T, et al. High-power all-solid-state batteries using sulfide superionic conductors. *Nat Energy* 2016;1. DOI
28. Ribes M, Barrau B, Souquet J. Sulfide glasses: glass forming region, structure and ionic conduction of glasses in Na_2SXS_2 (X Si;Ge), $\text{Na}_2\text{SP}_2\text{S}_5$ and $\text{Li}_2\text{S GeS}_2$ systems. *J Non-Crystall Solids* 1980;38-39:271-6. DOI
29. Rao M, Geng X, Li X, Hu S, Li W. Lithium-sulfur cell with combining carbon nanofibers-sulfur cathode and gel polymer electrolyte. *J Power Sources* 2012;212:179-85. DOI
30. Wang L, Wang YG, Xia YY. A high performance lithium-ion sulfur battery based on a Li_2S cathode using a dual-phase electrolyte. *Energy Environ Sci* 2015;8:1551-8. DOI
31. Shin BR, Nam YJ, Oh DY, Kim DH, Kim JW, Jung YS. Comparative study of $\text{TiS}_2/\text{Li-In}$ all-solid-state lithium batteries using glass-ceramic Li_3PS_4 and $\text{Li}_{10}\text{GeP}_2\text{S}_{12}$ solid electrolytes. *Electrochim Acta* 2014;146:395-402. DOI
32. Duan J, Wu W, Nolan AM, et al. Lithium-graphite paste: an interface compatible anode for solid-state batteries. *Adv Mater* 2019;31:e1807243. DOI PubMed
33. Wen J, Huang Y, Duan J, et al. Highly adhesive Li-BN nanosheet composite anode with excellent interfacial compatibility for solid-state Li metal batteries. *ACS Nano* 2019;13:14549-56. DOI PubMed
34. Ohara K, Mitsui A, Mori M, et al. Structural and electronic features of binary $\text{Li}_2\text{S-P}_2\text{S}_5$ glasses. *Sci Rep* 2016;6:21302. DOI PubMed PMC
35. Gao Z, Sun H, Fu L, et al. Promises, challenges, and recent progress of inorganic solid-state electrolytes for all-solid-state lithium batteries. *Adv Mater* 2018;30:e1705702. DOI PubMed
36. Zheng B, Zhu J, Wang H, et al. Stabilizing $\text{Li}_{10}\text{SnP}_2\text{S}_{12}/\text{Li}$ interface via an in situ formed solid electrolyte interphase layer. *ACS Appl Mater Interfaces* 2018;10:25473-82. DOI PubMed
37. Kraft MA, Culver SP, Calderon M, et al. Influence of lattice polarizability on the ionic conductivity in the lithium superionic argyrodites $\text{Li}_6\text{PS}_5\text{X}$ (X = Cl, Br, I). *J Am Chem Soc* 2017;139:10909-18. DOI PubMed
38. Das S, Ngeen P, Norby P, Vegge T, de Jongh PE, Blanchard D. All-solid-state lithium-sulfur battery based on a nanoconfined LiBH_4 electrolyte. *J Electrochem Soc* 2016;163:A2029-34. DOI
39. Fan Z, Ding B, Zhang T, et al. Solid/solid interfacial architecturing of solid polymer electrolyte-based all-solid-state lithium-sulfur batteries by atomic layer deposition. *Small* 2019;15:e1903952. DOI PubMed
40. Qu H, Zhang J, Du A, et al. Multifunctional sandwich-structured electrolyte for high-performance lithium-sulfur batteries. *Adv Sci (Weinh)* 2018;5:1700503. DOI PubMed PMC
41. Tatsumisago M. Glassy materials based on Li_2S for all-solid-state lithium secondary batteries. *Solid State Ionics* 2004;175:13-8. DOI
42. Hayashi A, Ohtomo T, Mizuno F, Tadanaga K, Tatsumisago M. Rechargeable lithium batteries, using sulfur-based cathode materials and $\text{Li}_2\text{S-P}_2\text{S}_5$ glass-ceramic electrolytes. *Electrochim Acta* 2004;50:893-7. DOI
43. Chen M, Prasada Rao R, Adams S. The unusual role of $\text{Li}_6\text{PS}_5\text{Br}$ in all-solid-state $\text{CuS}/\text{Li}_6\text{PS}_5\text{Br}/\text{In-Li}$ batteries. *Solid State Ionics* 2014;268:300-4. DOI
44. Li X, Liang J, Luo J, et al. High-performance Li-SeS_x all-solid-state lithium batteries. *Adv Mater* 2019;31:e1808100. DOI PubMed
45. Zhang Q, Huang N, Huang Z, Cai L, Wu J, Yao X. CNTs@S composite as cathode for all-solid-state lithium-sulfur batteries with ultralong cycle life. *J Energy Chem* 2020;40:151-5. DOI
46. Tatsumisago M, Nagao M, Hayashi A. Recent development of sulfide solid electrolytes and interfacial modification for all-solid-state rechargeable lithium batteries. *J Asian Cer Soc* 2013;1:17-25. DOI
47. Wang D, Wu Y, Zheng X, Tang S, Gong Z, Yang Y. $\text{Li}_2\text{S}@/\text{NC}$ composite enable high active material loading and high Li_2S utilization for all-solid-state lithium sulfur batteries. *J Power Sourc* 2020;479:228792. DOI
48. Wang Q, Chen Y, Jin J, Wen Z. A new high-capacity cathode for all-solid-state lithium sulfur battery. *Solid State Ionics* 2020;357:115500. DOI
49. Ando T, Sato Y, Matsuyama T, Sakuda A, Tatsumisago M, Hayashi A. High-rate operation of sulfur/mesoporous activated carbon composite electrode for all-solid-state lithium-sulfur batteries. *J Ceram Soc Japan* 2020;128:233-7. DOI
50. Phuc NHH, Takaki M, Muto H, Reiko M, Kazuhiro H, Matsuda A. Sulfur-carbon nano fiber composite solid electrolyte for all-solid-state Li-S batteries. *ACS Appl Energy Mater* 2020;3:1569-73. DOI
51. Shi J, Liu G, Weng W, et al. $\text{Co}_3\text{S}_4@/\text{Li}_7\text{P}_3\text{S}_{11}$ hexagonal platelets as cathodes with superior interfacial contact for all-solid-state lithium batteries. *ACS Appl Mater Interfaces* 2020;12:14079-86. DOI PubMed
52. Fujii Y, Kobayashi M, Miura A, et al. Fe-P-S electrodes for all-solid-state lithium secondary batteries using sulfide-based solid electrolytes. *J Power Sources* 2020;449:227576. DOI
53. Ryou M, Lee YM, Lee Y, Winter M, Bieker P. Mechanical surface modification of lithium metal: towards improved li metal anode performance by directed Li plating. *Adv Funct Mater* 2015;25:834-41. DOI
54. Kozen AC, Lin CF, Pearse AJ, et al. Next-generation lithium metal anode engineering via atomic layer deposition. *ACS Nano* 2015;9:5884-92. DOI PubMed
55. Kazyak E, Wood KN, Dasgupta NP. Improved cycle life and stability of lithium metal anodes through ultrathin atomic layer deposition surface treatments. *Chem Mater* 2015;27:6457-62. DOI
56. Yang CP, Yin YX, Zhang SF, Li NW, Guo YG. Accommodating lithium into 3D current collectors with a submicron skeleton towards long-life lithium metal anodes. *Nat Commun* 2015;6:8058. DOI PubMed PMC
57. Kwon O, Hirayama M, Suzuki K, et al. Synthesis, structure, and conduction mechanism of the lithium superionic conductor $\text{Li}_{10+\delta}\text{Ge}_{1+\delta}\text{P}_{2-\delta}\text{S}_{12}$. *J Mater Chem A* 2015;3:438-46. DOI

58. Liang Z, Lin D, Zhao J, et al. Composite lithium metal anode by melt infusion of lithium into a 3D conducting scaffold with lithiophilic coating. *Proc Natl Acad Sci USA* 2016;113:2862-7. DOI PubMed PMC
59. Cao Y, Meng X, Elam JW. Atomic layer deposition of Li XAl YS Solid-State Electrolytes for Stabilizing Lithium-Metal Anodes. *ChemElectroChem* 2016;3:858-63. DOI
60. Lin D, Liu Y, Liang Z, et al. Layered reduced graphene oxide with nanoscale interlayer gaps as a stable host for lithium metal anodes. *Nat Nano Technol* 2016;11:626-32. DOI PubMed
61. Liu Y, Lin D, Liang Z, Zhao J, Yan K, Cui Y. Lithium-coated polymeric matrix as a minimum volume-change and dendrite-free lithium metal anode. *Nat Commun* 2016;7:10992. DOI PubMed PMC
62. Sun Y, Zheng G, Seh Z, et al. Graphite-encapsulated Li-metal hybrid anodes for high-capacity Li batteries. *Chem* 2016;1:287-97. DOI
63. Zhang R, Cheng XB, Zhao CZ, et al. Conductive nanostructured scaffolds render low local current density to inhibit lithium dendrite growth. *Adv Mater* 2016;28:2155-62. DOI PubMed
64. Zhou W, Wang S, Li Y, Xin S, Manthiram A, Goodenough JB. Plating a dendrite-free lithium anode with a polymer/ceramic/polymer sandwich electrolyte. *J Am Chem Soc* 2016;138:9385-8. DOI PubMed
65. Pei A, Zheng G, Shi F, Li Y, Cui Y. Nanoscale Nucleation and growth of electrodeposited lithium metal. *Nano Lett* 2017;17:1132-9. DOI PubMed
66. Yang C, Yao Y, He S, Xie H, Hitz E, Hu L. Ultrafine silver nanoparticles for seeded lithium deposition toward stable lithium metal anode. *Adv Mater* 2017;29:1702714. DOI PubMed
67. Tao T, Lu S, Fan Y, Lei W, Huang S, Chen Y. Anode improvement in rechargeable lithium-sulfur batteries. *Adv Mater* 2017;29:1700542. DOI PubMed
68. Yu B, Tao T, Mateti S, Lu S, Chen Y. Nanoflake arrays of lithiophilic metal oxides for the ultra - stable anodes of lithium - metal batteries. *Adv Funct Mater* 2018;28:1803023. DOI
69. Sun Z, Jin S, Jin H, et al. Robust expandable carbon nanotube scaffold for ultrahigh-capacity lithium-metal anodes. *Adv Mater* 2018;30:e1800884. DOI PubMed
70. Zhang R, Wen S, Wang N, et al. N-doped graphene modified 3D porous Cu current collector toward microscale homogeneous Li deposition for Li metal anodes. *Adv Energy Mater* 2018;8:1800914. DOI
71. Zhang R, Chen X, Shen X, et al. Coraloid carbon fiber-based composite lithium anode for robust lithium metal batteries. *Joule* 2018;2:764-77. DOI
72. Zhou Y, Han Y, Zhang H, et al. A carbon cloth-based lithium composite anode for high-performance lithium metal batteries. *Energy Stor Mater* 2018;14:222-9. DOI
73. Zhang C, Liu S, Li G, Zhang C, Liu X, Luo J. Incorporating ionic paths into 3D conducting scaffolds for high volumetric and areal capacity, high rate lithium-metal anodes. *Adv Mater* 2018;30:e1801328. DOI PubMed
74. Huo H, Chen Y, Luo J, Yang X, Guo X, Sun X. Rational design of hierarchical “ceramic-in-polymer” and “polymer-in-ceramic” electrolytes for dendrite-free solid-state batteries. *Adv Energy Mater* 2019;9:1804004. DOI
75. Zhao Q, Liu X, Stalin S, Khan K, Archer LA. Solid-state polymer electrolytes with in-built fast interfacial transport for secondary lithium batteries. *Nat Energy* 2019;4:365-73. DOI
76. Xia Y, Liang Y, Xie D, et al. A poly (vinylidene fluoride-hexafluoropropylene) based three-dimensional network gel polymer electrolyte for solid-state lithium-sulfur batteries. *Chem Eng J* 2019;358:1047-53. DOI
77. Yang X, Luo J, Sun X. Towards high-performance solid-state Li-S batteries: from fundamental understanding to engineering design. *Chem Soc Rev* 2020;49:2140-95. DOI PubMed
78. Liu Y, Xu B, Zhang W, Li L, Lin Y, Nan C. Composition modulation and structure design of inorganic-in-polymer composite solid electrolytes for advanced lithium batteries. *Small* 2020;16:e1902813. DOI PubMed
79. Sun C, Liu J, Gong Y, Wilkinson DP, Zhang J. Recent advances in all-solid-state rechargeable lithium batteries. *Nano Energy* 2017;33:363-86. DOI
80. Chung H, Kang B. Mechanical and thermal failure induced by contact between a $\text{Li}_{1.5}\text{Al}_{0.5}\text{Ge}_{1.5}(\text{PO}_4)_3$ solid electrolyte and Li metal in an all solid-state Li cell. *Chem Mater* 2017;29:8611-9. DOI
81. Wenzel S, Leichtweiss T, Krüger D, Sann J, Janek J. Interphase formation on lithium solid electrolytes - an in situ approach to study interfacial reactions by photoelectron spectroscopy. *Solid State Ionics* 2015;278:98-105. DOI
82. Richards WD, Miara LJ, Wang Y, Kim JC, Ceder G. Interface stability in solid-state batteries. *Chem Mater* 2016;28:266-73. DOI
83. Eom M, Son S, Park C, Noh S, Nichols WT, Shin D. High performance all-solid-state lithium-sulfur battery using a Li_2S -VGCF nanocomposite. *Electrochim Acta* 2017;230:279-84. DOI PubMed
84. Yao X, Huang N, Han F, et al. High-performance all-solid-state lithium-sulfur batteries enabled by amorphous sulfur-coated reduced graphene oxide cathodes. *Adv Energy Mater* 2017;7:1602923. DOI
85. Sakuda A, Sato Y, Hayashi A, Tatsumisago M. Sulfur-based composite electrode with interconnected mesoporous carbon for all-solid-state lithium-sulfur batteries. *Energy Technol* 2019;7:1900077. DOI
86. Kamaya N, Homma K, Yamakawa Y, et al. A lithium superionic conductor. *Nat Mater* 2011;10:682-6. DOI PubMed
87. Liu ZC, Fu WJ, Payzant EA, et al. Anomalous high ionic conductivity of nanoporous $\beta\text{-Li}_3\text{PS}_4$. *J Am Chem Soc* 2013;135:975-8. DOI PubMed
88. Goodenough J, Kim Y. Challenges for rechargeable Li batteries. *Chem Mater* 2010;22:587-603. DOI

89. Whiteley JM, Woo JH, Hu E, Nam K, Lee S. Empowering the lithium metal battery through a silicon-based superionic conductor. *J Electrochem Soc* 2014;161:A1812-7. DOI
90. Zhu Y, He X, Mo Y. First principles study on electrochemical and chemical stability of solid electrolyte-electrode interfaces in all-solid-state Li-ion batteries. *J Mater Chem A* 2016;4:3253-66. DOI
91. Sicolo S, Fingerle M, Hausbrand R, Albe K. Interfacial instability of amorphous lipon against lithium: a combined density functional theory and spectroscopic study. *J Power Sources* 2017;354:124-33. DOI
92. Lei D, Shi K, Ye H, et al. Progress and perspective of solid-state lithium-sulfur batteries. *Adv Funct Mater* 2018;28:1707570. DOI
93. Sharafi A, Kazyak E, Davis AL, et al. Surface chemistry mechanism of ultra-low interfacial resistance in the solid-state electrolyte $\text{Li}_7\text{La}_3\text{Zr}_2\text{O}_{12}$. *Chem Mater* 2017;29:7961-8. DOI
94. Scheers J, Fantini S, Johansson P. A review of electrolytes for lithium-sulphur batteries. *J Power Sources* 2014;255:204-18. DOI
95. Jung YS, Oh DY, Nam YJ, Park KH. Issues and challenges for bulk-type all-solid-state rechargeable lithium batteries using sulfide solid electrolytes. *Isr J Chem* 2015;55:472-85. DOI
96. Cheng X, Zhao C, Yao Y, Liu H, Zhang Q. Recent advances in energy chemistry between solid-state electrolyte and safe lithium-metal anodes. *Chem* 2019;5:74-96. DOI
97. Pan H, Cheng Z, He P, Zhou H. A review of solid-state lithium-sulfur battery: ion transport and polysulfide chemistry. *Energy Fuels* 2020;34:11942-61. DOI
98. Sumita M, Tanaka Y, Ikeda M, Ohno T. Charged and discharged states of cathode/sulfide electrolyte interfaces in all-solid-state lithium ion batteries. *J Phys Chem C* 2016;120:13332-9. DOI
99. Xu R, Wu Z, Zhang S, et al. Construction of all-solid-state batteries based on a sulfur-graphene composite and $\text{Li}_{9.54}\text{Si}_{1.74}\text{P}_{1.44}\text{S}_{11.7}\text{Cl}_{0.3}$ solid electrolyte. *Chemistry* 2017;23:13950-6. DOI PubMed
100. Liu Y, He P, Zhou H. Rechargeable solid-state Li-Air and Li-S batteries: materials, construction, and challenges. *Adv Energy Mater* 2018;8:1701602. DOI
101. Riphaut N, Stiaszny B, Beyer H, Indris S, Gasteiger HA, Sedlmaier SJ. Editors' choice - understanding chemical stability issues between different solid electrolytes in all-solid-state batteries. *J Electrochem Soc* 2019;166:A975-83. DOI
102. Marceau H, Kim C, Paoletta A, et al. In operando scanning electron microscopy and ultraviolet-visible spectroscopy studies of lithium/sulfur cells using all solid-state polymer electrolyte. *J Power Sources* 2016;319:247-54. DOI
103. Chung S, Manthiram A. A Li_2S - TiS_2 -electrolyte composite for stable Li_2S -based lithium-sulfur batteries. *Adv Energy Mater* 2019;9:1901397. DOI PubMed
104. Xiang Y, Li X, Cheng Y, Sun X, Yang Y. Advanced characterization techniques for solid state lithium battery research. *Materials Today* 2020;36:139-57. DOI
105. Xu C, Sun B, Gustafsson T, Edström K, Brandell D, Hahlin M. Interface layer formation in solid polymer electrolyte lithium batteries: an XPS study. *J Mater Chem A* 2014;2:7256-64. DOI
106. Lin Y, Li J, Liu K, Liu Y, Liu J, Wang X. Unique starch polymer electrolyte for high capacity all-solid-state lithium sulfur battery. *Green Chem* 2016;18:3796-803. DOI
107. Li Y, Xu B, Xu H, et al. Hybrid polymer/garnet electrolyte with a small interfacial resistance for lithium-ion batteries. *Angew Chem Int Ed* 2017;56:753-6. DOI PubMed
108. Kim J. Hybrid gel polymer electrolyte for high-safety lithium-sulfur batteries. *Mater Lett* 2017;187:40-3. DOI
109. Hartmann P, Leichtweiss T, Busche MR, et al. Degradation of NASICON-type materials in contact with lithium metal: formation of mixed conducting interphases (MCI) on Solid electrolytes. *J Phys Chem C* 2013;117:21064-74. DOI
110. Wenzel S, Weber DA, Leichtweiss T, Busche MR, Sann J, Janek J. Interphase formation and degradation of charge transfer kinetics between a lithium metal anode and highly crystalline $\text{Li}_7\text{P}_3\text{S}_{11}$ solid electrolyte. *Solid State Ionics* 2016;286:24-33. DOI
111. Wang C, Gong Y, Liu B, et al. Conformal, nanoscale ZnO Surface modification of garnet-based solid-state electrolyte for lithium metal anodes. *Nano Lett* 2017;17:565-71. DOI PubMed
112. Xu B, Li W, Duan H, et al. Li_3PO_4 -added garnet-type $\text{Li}_{6.5}\text{La}_3\text{Zr}_{1.5}\text{Ta}_{0.5}\text{O}_{12}$ for Li-dendrite suppression. *J Power Sources* 2017;354:68-73. DOI
113. Sharafi A, Haslam CG, Kerns RD, Wolfenstine J, Sakamoto J. Controlling and correlating the effect of grain size with the mechanical and electrochemical properties of $\text{Li}_7\text{La}_3\text{Zr}_2\text{O}_{12}$ solid-state electrolyte. *J Mater Chem A* 2017;5:21491-504. DOI
114. Xia W, Xu B, Duan H, et al. Reaction mechanisms of lithium garnet pellets in ambient air: The effect of humidity and CO_2 . *J Am Ceram Soc* 2017;100:2832-9. DOI
115. Nagao M, Hayashi A, Tatsumisago M, et al. Li_2S nanocomposites underlying high-capacity and cycling stability in all-solid-state lithium-sulfur batteries. *J Power Sources* 2015;274:471-6. DOI
116. Xu R, Xia X, Li S, Zhang S, Wang X, Tu J. All-solid-state lithium-sulfur batteries based on a newly designed $\text{Li}_7\text{P}_{2.9}\text{Mn}_{0.1}\text{S}_{10.7}\text{I}_{0.3}$ superionic conductor. *J Mater Chem A* 2017;5:6310-7. DOI
117. Sheng O, Jin C, Luo J, et al. Ionic conductivity promotion of polymer electrolyte with ionic liquid grafted oxides for all-solid-state lithium-sulfur batteries. *J Mater Chem A* 2017;5:12934-42. DOI
118. Zhu P, Yan C, Zhu J, et al. Flexible electrolyte-cathode bilayer framework with stabilized interface for room-temperature all-solid-state lithium-sulfur batteries. *Energy Stor Mater* 2019;17:220-5. DOI
119. Shin M, Gewirth AA. Incorporating solvate and solid electrolytes for all-solid-state Li_2S batteries with high capacity and long cycle life. *Adv Energy Mater* 2019;9:1900938. DOI

120. Hayashi A, Ohtomo T, Mizuno F, Tadanaga K, Tatsumisago M. All-solid-state Li/S batteries with highly conductive glass-ceramic electrolytes. *Electr Comm* 2003;5:701-5. DOI
121. Zhu X, Wen Z, Gu Z, Lin Z. Electrochemical characterization and performance improvement of lithium/sulfur polymer batteries. *J Power Sources* 2005;139:269-73. DOI
122. Jeong S, Lim Y, Choi Y, et al. Electrochemical properties of lithium sulfur cells using PEO polymer electrolytes prepared under three different mixing conditions. *J Power Sources* 2007;174:745-50. DOI
123. Kobayashi T, Imade Y, Shishihara D, et al. All solid-state battery with sulfur electrode and thio-LISICON electrolyte. *J Power Sources* 2008;182:621-5. DOI
124. Hayashi A, Ohtsubo R, Ohtomo T, Mizuno F, Tatsumisago M. All-solid-state rechargeable lithium batteries with Li_2S as a positive electrode material. *J Power Sources* 2008;183:422-6. DOI
125. Hayashi A, Ohtsubo R, Nagao M, Tatsumisago M. Characterization of $\text{Li}_2\text{S}-\text{P}_2\text{S}_5$ -Cu composite electrode for all-solid-state lithium secondary batteries. *J Mater Sci* 2010;45:377-81. DOI
126. Nagao M, Hayashi A, Tatsumisago M. Sulfur-carbon composite electrode for all-solid-state Li/S battery with $\text{Li}_2\text{S}-\text{P}_2\text{S}_5$ solid electrolyte. *Electrochim Acta* 2011;56:6055-9. DOI
127. Nagao M, Hayashi A, Tatsumisago M. Fabrication of favorable interface between sulfide solid electrolyte and Li metal electrode for bulk-type solid-state Li/S battery. *Electr Comm* 2012;22:177-80. DOI
128. Agostini M, Aihara Y, Yamada T, Scrosati B, Hassoun J. A lithium-sulfur battery using a solid, glass-type P_2S_5 - Li_2S electrolyte. *Solid State Ionics* 2013;244:48-51. DOI
129. Nagao M, Imade Y, Narisawa H, et al. All-solid-state Li-sulfur batteries with mesoporous electrode and thio-LISICON solid electrolyte. *J Power Sources* 2013;222:237-42. DOI
130. Kinoshita S, Okuda K, Machida N, Shigematsu T. Additive effect of ionic liquids on the electrochemical property of a sulfur composite electrode for all-solid-state lithium-sulfur battery. *J Power Sources* 2014;269:727-34. DOI
131. Nagata H, Chikusa Y. Transformation of P_2S_5 into a solid electrolyte with ionic conductivity at the positive composite electrode of all-solid-state lithium-sulfur batteries. *Energy Technol* 2014;2:753-6. DOI
132. Chen M, Adams S. High performance all-solid-state lithium/sulfur batteries using lithium argyrodite electrolyte. *J Solid State Electrochem* 2015;19:697-702. DOI
133. Yu C, van Eijck L, Ganapathy S, Wagemaker M. Synthesis, structure and electrochemical performance of the argyrodite $\text{Li}_6\text{PS}_5\text{Cl}$ solid electrolyte for Li-ion solid state batteries. *Electrochim Acta* 2016;215:93-9. DOI
134. Choi HU, Jin JS, Park J, Lim H. Performance improvement of all-solid-state Li-S batteries with optimizing morphology and structure of sulfur composite electrode. *J Alloys Comp* 2017;723:787-94. DOI
135. Zhang Y, Chen K, Shen Y, Lin Y, Nan C. Synergistic effect of processing and composition x on conductivity of $x\text{Li}_2\text{S}-(100-x)\text{P}_2\text{S}_5$ electrolytes. *Solid State Ionics* 2017;305:1-6. DOI
136. Ulissi U, Ito S, Hosseini SM, Varzi A, Aihara Y, Passerini S. High capacity all-solid-state lithium batteries enabled by pyrite-sulfur composites. *Adv Energy Mater* 2018;8:1801462. DOI
137. Zhang Y, Liu T, Zhang Q, et al. High-performance all-solid-state lithium-sulfur batteries with sulfur/carbon nano-hybrids in a composite cathode. *J Mater Chem A* 2018;6:23345-56. DOI
138. Gracia I, Ben Youcef H, Judez X, et al. S-containing copolymer as cathode material in poly(ethylene oxide)-based all-solid-state Li-S batteries. *J Power Sources* 2018;390:148-52. DOI
139. Yu C, Hageman J, Ganapathy S, et al. Tailoring Li_6PS_5 Br ionic conductivity and understanding of its role in cathode mixtures for high performance all-solid-state Li-S batteries. *J Mater Chem A* 2019;7:10412-21. DOI
140. Lin Z, Liu Z, Fu W, Dudney NJ, Liang C. Lithium polysulfidophosphates: a family of lithium-conducting sulfur-rich compounds for lithium-sulfur batteries. *Angew Chem Int Ed* 2013;52:7460-3. DOI PubMed
141. Lin Z, Liu ZC, Dudney NJ, Liang CD. Lithium superionic sulfide cathode for all-solid lithium-sulfur batteries. *ACS Nano* 2013;7:2829-33. DOI PubMed
142. Unemoto A, Yasaku S, Nogami G, et al. Development of bulk-type all-solid-state lithium-sulfur battery using LiBH_4 electrolyte. *Appl Phys Lett* 2014;105:083901. DOI
143. Han F, Yue J, Fan X, et al. High-performance all-solid-state lithium-sulfur battery enabled by a mixed-conductive Li_2S nanocomposite. *Nano Lett* 2016;16:4521-7. DOI PubMed
144. Tao X, Liu Y, Liu W, et al. Solid-state lithium-sulfur batteries operated at 37 °C with composites of nanostructured $\text{Li}_7\text{La}_3\text{Zr}_2\text{O}_{12}$ /carbon foam and polymer. *Nano Lett* 2017;17:2967-72. DOI PubMed
145. Zhang C, Lin Y, Zhu Y, Zhang Z, Liu J. Improved lithium-ion and electrically conductive sulfur cathode for all-solid-state lithium-sulfur batteries. *RSC Adv* 2017;7:19231-6. DOI
146. Suzuki K, Kato D, Hara K, et al. Composite sulfur electrode prepared by high-temperature mechanical milling for use in an all-solid-state lithium-sulfur battery with a $\text{Li}_{3.25}\text{Ge}_{0.25}\text{P}_{0.75}\text{S}_4$ electrolyte. *Electrochim Acta* 2017;258:110-5. DOI
147. Suzuki K, Tateishi M, Nagao M, et al. Synthesis, structure, and electrochemical properties of a sulfur-carbon replica composite electrode for all-solid-state li-sulfur batteries. *J Electrochem Soc* 2017;164:A6178-83. DOI
148. Oh DY, Kim DH, Jung SH, Han J, Choi N, Jung YS. Single-step wet-chemical fabrication of sheet-type electrodes from solid-electrolyte precursors for all-solid-state lithium-ion batteries. *J Mater Chem A* 2017;5:20771-9. DOI
149. Trevey JE, Jung YS, Lee S. High lithium ion conducting $\text{Li}_2\text{S}-\text{GeS}_2-\text{P}_2\text{S}_5$ glass-ceramic solid electrolyte with sulfur additive for all

- solid-state lithium secondary batteries. *Electrochim Acta* 2011;56:4243-7. DOI
150. Hao Y, Wang S, Xu F, et al. A design of solid-state Li-S cell with evaporated lithium anode to eliminate shuttle effects. *ACS Appl Mater Interfaces* 2017;9:33735-9. DOI PubMed
151. Nagao M, Imade Y, Narisawa H, et al. Reaction mechanism of all-solid-state lithium-sulfur battery with two-dimensional mesoporous carbon electrodes. *J Power Sources* 2013;243:60-4. DOI
152. Zhu Y, Li J, Liu J. A bifunctional ion-electron conducting interlayer for high energy density all-solid-state lithium-sulfur battery. *J Power Sources* 2017;351:17-25. DOI
153. Zhang Q, Wan H, Liu G, Ding Z, Mwirerwa JP, Yao X. Rational design of multi-channel continuous electronic/ionic conductive networks for room temperature vanadium tetrasulfide-based all-solid-state lithium-sulfur batteries. *Nano Energy* 2019;57:771-82. DOI
154. Nagata H, Chikusa Y. An all-solid-state lithium-sulfur battery using two solid electrolytes having different functions. *J Power Sources* 2016;329:268-72. DOI
155. Hou L, Yuan H, Zhao C, et al. Improved interfacial electronic contacts powering high sulfur utilization in all-solid-state lithium-sulfur batteries. *Energy Stor Mater* 2020;25:436-42. DOI
156. Mo Y, Ong SP, Ceder G. First principles study of the $\text{Li}_{10}\text{GeP}_2\text{S}_{12}$ lithium super ionic conductor material. *Chem Mater* 2012;24:15-7. DOI
157. Sudo R, Nakata Y, Ishiguro K, et al. Interface behavior between garnet-type lithium-conducting solid electrolyte and lithium metal. *Solid State Ionics* 2014;262:151-4. DOI
158. Fu KK, Gong Y, Liu B, et al. Toward garnet electrolyte-based Li metal batteries: An ultrathin, highly effective, artificial solid-state electrolyte/metallic Li interface. *Sci Adv* 2017;3:e1601659. DOI PubMed PMC
159. Sakuma M, Suzuki K, Hirayama M, Kanno R. Reactions at the electrode/electrolyte interface of all-solid-state lithium batteries incorporating Li-M (M = Sn, Si) alloy electrodes and sulfide-based solid electrolytes. *Solid State Ionics* 2016;285:101-5. DOI
160. Yang C, Xie H, Ping W, et al. An Electron/Ion dual-conductive alloy framework for high-rate and high-capacity solid-state lithium-metal batteries. *Adv Mater* 2019;31:e1804815. DOI PubMed
161. Kato A, Hayashi A, Tatsumisago M. Enhancing utilization of lithium metal electrodes in all-solid-state batteries by interface modification with gold thin films. *J Power Sources* 2016;309:27-32. DOI
162. Shen X, Li Y, Qian T, et al. Lithium anode stable in air for low-cost fabrication of a dendrite-free lithium battery. *Nat Commun* 2019;10:900. DOI PubMed PMC
163. Han X, Gong Y, Fu KK, et al. Negating interfacial impedance in garnet-based solid-state Li metal batteries. *Nat Mater* 2017;16:572-9. DOI PubMed
164. Cheng Q, Li A, Li N, et al. Stabilizing solid electrolyte-anode interface in li-metal batteries by boron nitride-based nanocomposite coating. *Joule* 2019;3:1510-22. DOI
165. Luo W, Gong Y, Zhu Y, et al. Reducing interfacial resistance between garnet-structured solid-state electrolyte and Li-metal anode by a germanium layer. *Adv Mater* 2017;29:1606042. DOI PubMed
166. Luo W, Gong Y, Zhu Y, et al. Transition from superlithiophobicity to superlithiophilicity of garnet solid-state electrolyte. *J Am Chem Soc* 2016;138:12258-62.
167. Shao Y, Wang H, Gong Z, et al. Drawing a soft interface: an effective interfacial modification strategy for garnet-type solid-state li batteries. *ACS Energy Lett* 2018;3:1212-8. DOI
168. Sun B, Jin Y, Lang J, Liu K, Fang M, Wu H. A painted layer for high-rate and high-capacity solid-state lithium-metal batteries. *Chem Commun* 2019;55:6704-7. DOI PubMed
169. Zhang Z, Chen S, Yang J, et al. Interface re-engineering of $\text{Li}_{10}\text{GeP}_2\text{S}_{12}$ electrolyte and lithium anode for all-solid-state lithium batteries with ultralong cycle life. *ACS Appl Mater Interfaces* 2018;10:2556-65. DOI PubMed
170. Kızılaslan A, Akbulut H. Assembling all-solid-state lithium-sulfur batteries with Li_3N -protected anodes. *Chempluschem* 2019;84:183-9. DOI PubMed
171. Li S, Ruan J, Jiang R, et al. Inorganic all-solid-state lithium-sulfur batteries enhanced by facile thermal formation. *Energy Stor Mater* 2022;48:283-9. DOI
172. Zhong L, Wang S, Xiao M, et al. Addressing interface elimination: Boosting comprehensive performance of all-solid-state Li-S battery. *Energy Stor Mater* 2021;41:563-70. DOI
173. Zhang Z, Zhao Y, Chen S, et al. An advanced construction strategy of all-solid-state lithium batteries with excellent interfacial compatibility and ultralong cycle life. *J Mater Chem A* 2017;5:16984-93. DOI
174. Yang H, Zhang Y, Tennenbaum MJ, et al. Polypropylene carbonate-based adaptive buffer layer for stable interfaces of solid polymer lithium metal batteries. *ACS Appl Mater Interfaces* 2019;11:27906-12. DOI PubMed
175. Yu Q, Han D, Lu Q, et al. Constructing effective interfaces for $\text{Li}_{1.5}\text{Al}_{0.5}\text{Ge}_{1.5}(\text{PO}_4)_3$ pellets to achieve room-temperature hybrid solid-state lithium metal batteries. *ACS Appl Mater Interfaces* 2019;11:9911-8. DOI PubMed
176. Zhou F, Li Z, Lu YY, et al. Diatomite derived hierarchical hybrid anode for high performance all-solid-state lithium metal batteries. *Nat Commun* 2019;10:2482.
177. Yuan H, Nan H, Zhao C, et al. Cover feature: slurry-coated sulfur/sulfide cathode with li metal anode for all-solid-state lithium-sulfur pouch cells. *Batteries Supercaps* 2020;3:568-568. DOI
178. Jafta CJ, Prévost S, He L, et al. Quantifying the chemical, electrochemical heterogeneity and spatial distribution of (poly) sulfide

- species using operando SANS. *Energy Stor Mater* 2021;40:219-28. DOI
179. Zhu Z, Lu LL, Yin Y, Shao J, Shen B, Yao HB. High rate and stable solid-state lithium metal batteries enabled by electronic and ionic mixed conducting network interlayers. *ACS Appl Mater Interfaces* 2019;11:16578-85. DOI PubMed
180. Gao X, Zheng X, Tsao Y, et al. All-solid-state lithium-sulfur batteries enhanced by redox mediators. *J Am Chem Soc* 2021;143:18188-95. DOI PubMed
181. Duan C, Cheng Z, Li W, et al. Realizing the compatibility of a Li metal anode in an all-solid-state Li-S battery by chemical iodine-vapor deposition. *Energy Environ Sci* 2022;15:3236-45. DOI
182. Liu S, Wang H, Imanishi N, et al. Effect of co-doping nano-silica filler and N-methyl-N-propylpiperidinium bis(trifluoromethanesulfonyl)imide into polymer electrolyte on Li dendrite formation in Li/poly(ethylene oxide)-Li(CF₃SO₂)₂N/Li. *J Power Sources* 2011;196:7681-6. DOI
183. Liu W, Liu N, Sun J, et al. Ionic conductivity enhancement of polymer electrolytes with ceramic nanowire fillers. *Nano Lett* 2015;15:2740-5. DOI PubMed
184. Fu KK, Gong Y, Dai J, et al. Flexible, solid-state, ion-conducting membrane with 3D garnet nanofiber networks for lithium batteries. *Proc Natl Acad Sci USA* 2016;113:7094-9. DOI PubMed PMC
185. Wang Q, Wen Z, Jin J, et al. A gel-ceramic multi-layer electrolyte for long-life lithium sulfur batteries. *Chem Commun* 2016;52:1637-40. DOI PubMed
186. Blanga R, Goor M, Burstein L, et al. The search for a solid electrolyte, as a polysulfide barrier, for lithium/sulfur batteries. *J Solid State Electrochem* 2016;20:3393-404. DOI
187. Xia Y, Wang X, Xia X, et al. A newly designed composite gel polymer electrolyte based on poly(vinylidene fluoride-hexafluoropropylene) (PVDF-HFP) for enhanced solid-state lithium-sulfur batteries. *Chemistry* 2017;23:15203-9. DOI PubMed
188. Liu W, Lee SW, Lin D, et al. Enhancing ionic conductivity in composite polymer electrolytes with well-aligned ceramic nanowires. *Nat Energy* 2017;2. DOI
189. Judez X, Zhang H, Li C, et al. Lithium bis(fluorosulfonyl)imide/poly(ethylene oxide) Polymer electrolyte for all solid-state Li-S cell. *J Phys Chem Lett* 2017;8:1956-60. DOI PubMed
190. Wenzel S, Sedlmaier SJ, Dietrich C, Zeier WG, Janek J. Interfacial reactivity and interphase growth of argyrodite solid electrolytes at lithium metal electrodes. *Solid State Ionics* 2018;318:102-12. DOI
191. Chen L, Li Y, Li S, Fan L, Nan C, Goodenough JB. PEO/garnet composite electrolytes for solid-state lithium batteries: From “ceramic-in-polymer” to “polymer-in-ceramic”. *Nano Energy* 2018;46:176-84. DOI
192. Lee J, Howell T, Rottmayer M, Boeckl J, Huang H. Free-standing PEO/LITFSI/LAGP composite electrolyte membranes for applications to flexible solid-state lithium-based batteries. *J Electrochem Soc* 2019;166:A416-22. DOI
193. Xu X, Hou G, Nie X, et al. Li₇P₃S₁₁/poly(ethylene oxide) hybrid solid electrolytes with excellent interfacial compatibility for all-solid-state batteries. *J Power Sources* 2018;400:212-7. DOI
194. Hu J, Yuan H, Yang S, et al. Dry electrode technology for scalable and flexible high-energy sulfur cathodes in all-solid-state lithium-sulfur batteries. *J Energy Chem* 2022;71:612-8. DOI
195. Dai J, Yang C, Wang C, Pastel G, Hu L. Interface engineering for garnet-based solid-state lithium-metal batteries: materials, structures, and characterization. *Adv Mater* 2018;30:e1802068. DOI PubMed
196. Nobili F, Tossici R, Marassi R, Croce F, Scrosati B. An AC impedance spectroscopic study of Li_xCoO₂ at different temperatures. *J Phys Chem B* 2002;106:3909-15. DOI
197. Zhang W, Weber DA, Weigand H, et al. Interfacial processes and influence of composite cathode microstructure controlling the performance of all-solid-state lithium batteries. *ACS Appl Mater Interfaces* 2017;9:17835-45. DOI PubMed
198. Wang C, Gong Y, Dai J, et al. In situ neutron depth profiling of lithium metal-garnet interfaces for solid state batteries. *J Am Chem Soc* 2017;139:14257-64. DOI PubMed
199. Ishiguro K, Nakata Y, Matsui M, et al. Stability of Nb-Doped Cubic Li₇La₃Zr₂O₁₂ with Lithium Metal. *J Electrochem Soc* 2013;160:A1690-3. DOI
200. Schwöbel A, Hausbrand R, Jaegermann W. Interface reactions between LiPON and lithium studied by in-situ X-ray photoemission. *Solid State Ionics* 2015;273:51-4. DOI
201. Gong Y, Zhang J, Jiang L, et al. In situ atomic-scale observation of electrochemical delithiation induced structure evolution of LiCoO₂ Cathode in a working all-solid-state battery. *J Am Chem Soc* 2017;139:4274-7. DOI PubMed
202. Yousaf M, Naseer U, Li Y, et al. A mechanistic study of electrode materials for rechargeable batteries beyond lithium ions by in situ transmission electron microscopy. *Energy Environ Sci* 2021;14:2670-707. DOI
203. Nagao M, Hayashi A, Tatsumisago M, Kanetsuku T, Tsuda T, Kuwabata S. In situ SEM study of a lithium deposition and dissolution mechanism in a bulk-type solid-state cell with a LiS-P₂S₅ solid electrolyte. *Phys Chem Chem Phys* 2013;15:18600-6. DOI
204. Tan DHS, Banerjee A, Chen Z, Meng YS. From nanoscale interface characterization to sustainable energy storage using all-solid-state batteries. *Nat Nanotechnol* 2020;15:170-80. DOI PubMed
205. Liang X, Wang L, Wu X, et al. Solid-state electrolytes for solid-state lithium-sulfur batteries: comparisons, advances and prospects. *J Energy Chem* 2022;73:370-86. DOI
206. Li G, Chen Z, Lu J. Lithium-sulfur batteries for commercial applications. *Chem* 2018;4:3-7. DOI
207. Zhu B, Mi Y, Xia C, et al. A nanoscale perspective on solid oxide and semiconductor membrane fuel cells: materials and technology. *Energy Mater* 2022;1:100002. DOI